HITACHI

GE Hitachi Nuclear Energy

3901 Castle Hayne Road, Wilmington, NC 28401

Licensing Topical Report

ESBWR
CONTAINMENT LOAD DEFINITION

NON-PROPRIETARY INFORMATION NOTICE

This is a non-proprietary version of the document NEDE-33261P, which has the proprietary information removed. Portions of the document that have been removed are indicated by open and closed double brackets as shown here [[   ]].

Important Notice Regarding Contents of this Report

Please read carefully

The information contained in this document is furnished for the purpose of obtaining NRC approval of the ESBWR Certification and implementation. The only undertakings of GE Hitachi Nuclear Energy with respect to information in this document are contained in contracts between GE Hitachi Nuclear Energy and participating utilities, and nothing contained in this document shall be construed as changing those contracts. The use of this information by anyone other than that for which it is intended is not authorized; and with respect to **any unauthorized use**, GE Hitachi Nuclear Energy makes no representation or warranty, and assumes no liability as to the completeness, accuracy, or usefulness of the information contained in this document.

TABLE OF CONTENTS

Title   **Page**

TABLE OF CONTENTS

Title   **Page**

LIST OF TABLES

LIST OF FIGURES

ACRONYMS AND ABBREVIATIONS

Term	Definition
ABWR	Advanced Boiling Water Reactor
ADS	Automatic Depressurization System
ANS / ANSI	American Nuclear Standard / American Nuclear Standards Institute
BOP	Balance of Plant
BWR	Boiling Water Reactor
CH	Chugging
CLD	Containment Load Definition
CO	Condensation Oscillation
COL	Combined Operating License
DBA	Design Basis Accident
DPV	Depressurization Valve
DW	Drywell
FS*	Partial Full-Scale
FSI	Fluid-Structure Interactions
FWLB	Feedwater Line Break
GDCS	Gravity Driven Cooling System
GE	General Electric Company
GEH	GE Hitachi Nuclear Energy
GESSAR	General Electric Standard Safety Analysis Report
HEM	Homogeneous Equilibrium Model
HVT	Horizontal Vent Test
HWL	High Water Level
IBA	Intermediate Break Accident
ICS	Isolation Condenser System
LOCA	Loss-of-Coolant Accident
LWL	Low Water Level
MSIV	Main Steam Isolation Valve
MSLB	Main Steam Line Break
PCCS	Passive Containment Cooling System
PS	Pool Swell
PSD	Power Spectral Density
PSTF	Pressure Suppression Test Facility
RMS	Root Mean Square
RPV	Reactor Pressure Vessel
S/P	Suppression Pool
SBA	Small Break Accident
SRSS	Square Root of the Sum of the Squares
SRV	Safety Relief Valve
SRVDL	Safety Relief Valve Discharge Line
SS	Sub-Scale
SST	Sub-Scaled Test
SV	Safety Valve
WW	Wetwell

Abstract

The ESBWR Containment Load Definition (CLD) provides a description and load definition methodology for hydrodynamic loading conditions inside the primary containment in an ESBWR during a postulated LOCA and/or a SRV or DPV actuation. The hydrodynamic loads covered by the CLD include pool swell, condensation oscillation, chugging, and SRV bubble pressure loads. The ESBWR containment load definition methodology used is similar to that used for prior BWR pressure suppression containment designs, such as the Advanced Boiling Water Reactor. The hydrodynamic loads calculated by this methodology are combined with other loads in the structural evaluation of the plant.

1.0   SCOPE

The ESBWR Containment Load Definition (CLD) provides a description and load definition methodology for hydrodynamic loading conditions inside the primary containment in an ESBWR during a postulated Loss-of-Coolant Accident (LOCA) and/or a Safety Relief Valve (SRV) or Depressurization Valve (DPV) actuation. Overall, the load definition methodology used for the ESBWR containment design is similar to that used for prior BWR containment designs, such as the Advanced Boiling Water Reactor (ABWR, Reference 1).

Any loads classified as minor, such as froth impingement or pool swell fall back, are not specified due to their insignificant impact on the structure.

2.0   DESCRIPTION OF PHENOMENA

This section describes the assumed sequence of events for loads evaluation during a postulated LOCA event and/or an SRV/DPV actuation.   This section also describes the potential containment loading conditions over the spectrum of LOCA break sizes and SRV/DPV actuation circumstances. The load combinations for the design evaluation are discussed in Section 9.0.

2.1   Loss-of-Coolant Accident

A Loss-of-Coolant Accident (LOCA) causes a pressure and temperature transient in the drywell and wetwell due to mass and energy released to the drywell. The severity of this transient loading condition depends upon the type and size of LOCA.

2.1.1   Large Break Accident (Design Basis Accident)

Because the ESBWR has no recirculation lines, the main steam line break and the feedwater line break become the large break cases. In these breaks, the upper drywell pressure increases as a result of the mass and energy release from the break, and a steam-nitrogen[a] mixture is forced through the main vent system. The water initially contained in the vent system is accelerated out of the horizontal vents. During the horizontal vent clearing process, the water exiting the vents form submerged jets in the suppression pool, which can produce loads on structures near the vent exits and on the containment wall opposite the vents.

Immediately following the water clearing, bubbles containing nitrogen and steam form at the horizontal vent exits. As the flow of nitrogen and steam from the drywell becomes established in the vent system, the initial bubbles at the horizontal vent exits expand. These bubbles possess a pressure nearly equal to the drywell pressure plus the hydrostatic pressure. The steam fraction of the flow into the pool is condensed, but the continuous injection of drywell nitrogen and the resultant expansion of the nitrogen bubbles produces a rapid rise of the suppression pool surface. This phenomenon is called Pool Swell (PS). The expanding bubble causes loads on both submerged structures and the suppression pool boundaries.

During the early stages of PS, a slug of water above the top vent is accelerated upward by the expanding nitrogen bubble. Structures and equipment close to the pool surface experience impact loads as the rising pool surface hits the bottom surface of the structures. Along with these impact loads, dissipative drag loads develop as water flows past structures and equipment at elevations above the vent exit and below the maximum PS height. This rising and expanding bubble eventually breaks through the water ligament and communicates with the wetwell airspace. Breakthrough occurs when the instabilities formed in the rising ligament cause the

---

[a] All references to "nitrogen" imply non-condensable gases.

surface to become unstable and shatter. Froth continues upward until decelerated to zero velocity by gravity. A PS impact load on the diaphragm floor does not occur due to increasing wetwell gas space pressure.

Following the PS transient, a period of high steam flow rate through the horizontal vent system commences. As the reactor blowdown progresses, the flow rate through the horizontal vent system decreases. Overall, prior test data have indicated that the steam is condensed in the horizontal vent exit region.

The steam condensation process at the vent exit is influenced by the horizontal vent steam mass flow rate, the subcooling at the vent exit, and the vent flow nitrogen content fraction. At medium vent flow rates, the water-to-steam condensation interface oscillates causing pressure oscillations in the pool. This phenomenon, referred to as Condensation Oscillation (CO), produces oscillatory and steady loadings on the containment structure.

As the vessel blowdown continues, the vent flow rate decreases and the vent flow nitrogen content becomes negligibly small. At lower vent flow rates (below a threshold level) the steam bubble at the vent exit alternatively grows, and, then nearly instantaneously collapses, in a condensation process referred to as chugging (CH). The CH process produces transient dynamic loading on the vents and the suppression pool boundary, which must be considered in the design evaluation of the containment system.

As the LOCA event progresses, the Automatic Depressurization System (ADS) is initiated. After a preset time delay, the first set of SRVs automatically opens. This allows for an additional vessel depressurization path, which is routed directly to the suppression pool. Following another preset time delay, a second set of SRVs automatically opens. This provides for additional depressurization capacity to the suppression pool. After another preset time delay, a set of DPVs automatically opens. These DPVs allow for depressurization directly to the drywell. This sequence repeats itself until all the DPVs are open. At the point where the pressure of the drywell plus the gravitational head in the Gravity Driven Cooling System (GDCS) exceeds that of the Reactor Pressure Vessel (RPV), low-pressure coolant begins to flow into the vessel.

The Passive Containment Cooling System (PCCS) would serve to mitigate the PS loads calculated for the scenario described above. In the ESBWR, the PCCS receives a steam-gas mixture supply directly from the drywell. Because the PCCS does not have any valves, it is in operation immediately following a LOCA. Nitrogen, together with steam, enters the PCCS condenser; steam is condensed inside the PCCS condenser tubes, and the nitrogen is purged to the wetwell.

2.1.2 Intermediate Break Accident

The Intermediate Break Accident (IBA) is defined as a break size such that rapid depressurization of the RPV does not occur due to break flow. However, the reactor inventory loss is sufficiently rapid to cause a reduction in the reactor water level.

An IBA increases drywell pressure and temperature at a moderate rate, compared to that due to a large break Design Basis Accident (DBA). However, the hydrodynamic phenomenon is similar to DBA. Water initially contained in the vent system is accelerated from the vents. During the vent clearing process, the water exiting the vents forms water jets in the suppression pool, which cause loads on the submerged structures and equipment near the vent exits. The containment and submerged structure loads from an IBA are less severe than those from a DBA.

Immediately following vent water clearing, nitrogen and steam bubbles form at the vent exits. The drywell pressurization rate for an IBA is less than that due to a DBA. Consequently, the bubble pressure in the suppression pool is less severe and the moderate rate of drywell pressurization does not result in significant PS. The resulting IBA loads on pool boundaries, submerged structures, and equipment are bounded by the corresponding loads from a DBA.

A high drywell pressure signal scrams the reactor during the IBA. The sequence of events following the scram can lead to closure of the main steamline isolation valves (MSIVs) and subsequent increase in RPV pressure. The Isolation Condenser System (ICS) would control the RPV pressure increase. However, for loads evaluation, no credit is taken for the ICS. It is assumed that the pressure is relieved by opening the SRVs and the DPVs as in the DBA ADS function. SRV and DPV discharges may continue intermittently to regulate reactor pressure and remove decay heat. Consequently, the suppression pool boundary may be subjected to a pressure loading resulting from the SRV and DPV discharges during IBA.

For intermediate size breaks, the CO loads are equal to or less severe than those during a DBA. Therefore, the DBA CO load is used for IBA. Following nitrogen carryover, however, CH loads, similar to the DBA, are experienced until the reactor vessel blowdown is reduced to a flow rate where CH becomes insignificant.

2.1.3 Small Break Accident

The Small Break Accident (SBA) is defined as an event in which the fluid loss from the RPV is insufficient to either depressurize the reactor or result in a rapid decrease of reactor water level. Following the break, the drywell pressure slowly increases until the high drywell pressure scram setting is reached.

Consequently, the drywell pressure continues to increase at a rate dependent upon the size of the postulated break. The pressure increase depresses the water level in the vent system until the water is expelled and the nitrogen and steam mixture enters the suppression pool. The nitrogen flow rate is such that the nitrogen bubbles through the pool without causing any appreciable PS. The steam is condensed, and the drywell nitrogen passes through the pool into the wetwell gas-space. The wetwell gas-space gradually pressurizes at a rate dependent upon the nitrogen carryover rate, which in turn, depends upon the break size. Eventually, the steam and nitrogen flow through the vents transfers essentially all the drywell nitrogen to the wetwell gas space.

During SBA, the ADS operation occurs following a low level signal in the RPV. The DPV actuation provides a direct steam flow path from the RPV to the upper drywell. Thus, the operation of the DPVs increases the mass flux through the main vents and transforms the SBA into a subset of the DBA LOCA. Because the DBA LOCA vent mass flux bounds the SBA LOCA vent mass flux, the PS, CO, and CH loads calculated for the DBA LOCA are used for design.

2.2 Safety Relief Valve Discharge

Safety Relief Valves (SRVs) and Safety Valves (SVs) are utilized in ESBWR to provide pressure relief during certain reactor transients. Steam blowdown through the SRVs is routed through discharge lines into the pressure suppression pool, where it is condensed. At the end of each discharge line is a quencher. The X-quencher discharge device promotes effective heat transfer and stable condensation of discharged steam in the suppression pool.

Each SRV is routed to a separate quencher.

The SVs discharge through rupture disks to the drywell. The impact on containment loads for SV discharge is described in Section 2.3.

SRV or SV actuation may occur for the following reasons:

- Pressure Actuation—For LOCA, five SRVs open at RPV Level 1 set-point and five SRVs open with a preset delay.
- Overpressure Protection – If the RPV pressure increases to the spring set-point of the valves (SRV or SV), the valve opens.
- Manual Operation—A planned operator action resulting in the opening of anywhere from one to ten Automatic Depressurization System (ADS) SRVs.
- Inadvertent Opening—A failure or error affecting one SRV or SV resulting in the opening of a single valve.

The discharge piping of an SRV contains ambient nitrogen and a column of water whose height is determined by the submergence of the SRV discharge line in the suppression pool and the pressure difference. Upon actuation, pressure builds up inside the piping as steam compresses the nitrogen and forces the water column through the quencher into the suppression pool.

The expulsion of water from the discharge line into the suppression pool is called the water-clearing phase of the discharge. The loads associated with the water clearing are:

- Transient pipe pressure and thermal loads.
- Pipe reaction forces from transient pressure waves and fluid motion in the pipe.
- Drag loads on structures located in the path of the submerged water jet.
- Pool boundary loads.

Following the expulsion of the water from the quencher, the nitrogen is expelled into the suppression pool in the form of high-pressure bubbles. Once the nitrogen bubbles are in the suppression pool, they expand because the ambient suppression pool pressure is lower than the nitrogen bubble pressure. The subsequent interaction of the nitrogen bubbles and the suppression pool manifests itself as an oscillatory pressure field, which persists with decaying amplitude until the nitrogen bubble rises to the suppression pool surface. The frequency of the pressure oscillation is influenced by the initial mass of nitrogen in the line, the submergence of the discharge line in the pool, the suppression pool temperature, the pool geometry and the wetwell gas space pressure. The loads associated with the nitrogen bubble dynamic phenomena are transient drag loads on submerged structures caused by the velocity field (standard drag) and the acceleration field (inertial drag), and oscillating pressure loads on the pool boundary.

Following the nitrogen-clearing phase, a steady discharge flow is established and continues until the valve is closed. The steam enters the pool from the quencher as a submerged jet emanating from multiple small holes in each quencher arm. The loads associated with the steady steam flow phase of the SRV discharge include:

- Pipe reaction forces caused by the steady steam flow through the pipe bends.
- Thrust forces on the quencher.
- Thermal loads on structures contacted by the steam.
- Pool boundary loads caused by the oscillation of the condensing steam jets at the quencher.

Following SRV closure, the steam in the discharge line condenses, and the resulting vacuum draws water back into the line. To limit the water level rise within the pipe, vacuum breakers are provided to admit drywell nitrogen to the discharge line and allow the water level to return to near normal.

For multiple SRV discharge conditions, the basic discharge line clearing phenomena are the same as those described for a single discharge. The loads in the suppression pool are the result of the combined effects of the discharges at a number of locations in the suppression pool.

2.3 Depressurization Valve Actuation

Depressurization Valves (DPVs) are part of the ADS, in conjunction with the SRVs. When low water level is signaled, the reactor is automatically depressurized by SRVs in combination with the DPVs.

The operation of the DPVs or SVs increases the mass flux through the main vents; however, the DBA LOCA vent mass flux is the bounding mass flux. Therefore, for containment hydrodynamic loads (PS, CO, and CH), the loads calculated for DBA LOCA are used for design.

3.0   POOL SWELL LOAD

The phenomena of Vent Clearing and Pool Swell (PS) that occur following a postulated DBA, are described in Section 2.1.1. The PS related loads are evaluated using computational models that determine mass and energy flow into the suppression pool, and the swelling of the suppression pool water surface. No credit is taken for the operation of the Isolation Condenser System (ICS) and the Passive Containment Cooling System (PCCS) for calculating the PS related loads. The dominant loads that require consideration with this phenomenon are:

- The pool boundary loads and loads on submerged structures due to the nitrogen bubble formation.
- Wetwell nitrogen compression boundary loads due to the PS.
- Diaphragm floor pressure load due to wetwell gas-space pressurization.
- Impact and drag loads on the wetwell gas-space internal structures initially above the pool surface.

3.1   Pool Swell (PS) Analytical Model

3.1.1   Drywell Pressurization

Both a main steam line break (MSLB) and feedwater line break (FWLB) are evaluated for pool swell. The maximum drywell pressurization rate occurs during an instantaneous guillotine rupture of a main steam line; therefore, the PS loads for the MSLB bound the loads for the FWLB.

For the MSLB, the ESBWR short-term containment pressurization model (Reference 2) is the same model utilized in earlier GE pressure suppression containment types, including the ABWR (Reference 1). The model consists of three main modules: the vessel blowdown model, the drywell model and the wetwell model.

Immediately following an instantaneous guillotine rupture of a main steam line, flow from both ends of the break accelerates to the maximum determined by critical flow considerations. Unsteady flow from the RPV side initially depletes the pipe inventory, and thereafter the flow corresponds to a steady critical flow in the flow restrictor in the steam nozzle. Blowdown flow through the Balance of Plant (BOP) side of the break occurs because the steam lines are interconnected at a point upstream of the turbine by a header. This interconnection allows primary system fluid to flow from the unbroken steamline, through the header and back into the drywell (DW) via the broken line, until the MSIVs are fully closed. Once the MSIVs are closed, the break flow is only from the RPV through the broken line.

In modeling the MSLB; the following major assumptions are made:

1. The reactor is operating at 102% of rated thermal power (4500 MWt) and the initial dome pressure is 1055 psia.
2. Reactor scram occurs at time zero.
3. Moody's HEM break flow model is assumed.
4. The GDCS, ICS, and PCCS systems are not modeled in the analysis.
5. Drywell and wetwell airspace are homogeneous mixtures of inert atmosphere, vapor and liquid water.
6. Wetwell and drywell structure heat transfer are not modeled.
7. The safety relief valves (SRV) and depressurization valves (DPV) are not modeled in the analysis.
8. Non-safety cooling systems are not modeled.
9. The drywell is modeled as a single node and all break flow into the drywell is homogeneously mixed with the drywell inventory.
10. The ANSI/ANS-5-1971 +20%/+10% decay heat is used.
11. The wetwell airspace and suppression pool are in thermal equilibrium.
12. The flow loss coefficient for the vent filter at the entrance to the main vertical vents is taken as 0.2.
13. Because of the unique containment geometry of ESBWR, in the event of a pipe break in the upper DW, the inert atmosphere in the lower DW would not start transferring to the wetwell (WW) until the peak pressure in the upper DW is achieved. Because the lower DW is connected to the upper DW through openings in the vessel support, no gas can escape from the lower DW until the peak pressure occurs. The contents of the lower DW starts transferring to the WW as soon as the pressure starts decreasing. A conservative transfer of 50% of the lower DW contents into the WW is assumed, by modeling the upper DW and lower DW regions as a single volume node comprising of the upper DW volume plus 50% of the lower DW volume.
14. MSIVs begin to close at 0.5 seconds after event initiation and fully close in the maximum time (5 seconds). This assumption of a closure time of 5.0 seconds, which maximizes the calculated discharge of high-energy fluid to the DW, is used for conservatism.
15. The flow resistance of open MSIVs is considered. The effective flow area on the BOP side reduces to 70% of a frictionless piping area.
16. During the inventory depletion period, a 0.75 flow multiplier is applied (Reference 2).
17. The break flow is steam for two seconds followed by a two-phase mixture. The 2-second delay in RPV level swell results in the maximum PS pressure response.

3.1.2   Hydrodynamic Loads

The hydrodynamic loads during the pool swell phase of LOCA are determined using an analytical model described in Reference 3. The analytical model is the same model reviewed and accepted for ABWR (Reference 1), which has a similar containment suppression pool and

vent system design.   Both ESBWR and ABWR have an annular suppression pool with a rectangular cross-section. The drywell and suppression pool are connected by a set of circular vertical vents each containing three circular horizontal vents. The horizontal and vertical vent diameters are the same for both designs. The horizontal vent elevations are the same for the two designs.

This analytical model is used to compute the pool boundary loads due to bubble formation, the pool swell velocity and acceleration, the pool surface elevation, and the wetwell airspace pressure. The assumptions inherent in the model maximize the nitrogen bubble pressure and, consequently, the pool swell velocity. The conservatism of the model in predicting PS velocity and wetwell gas-space pressure has been demonstrated for prior BWR plants.

In modeling and simulating the pool swell phenomenon, the following major assumptions are made:

1. Nitrogen is assumed to follow ideal gas laws.
2. Flow into the vent pipe following vent clearing is limited to nitrogen only.
3. The flow rate of nitrogen in the vent pipe is calculated assuming one-dimensional flow under adiabatic conditions while taking the pipe friction into consideration.
4. The nitrogen in the drywell is compressed isentropically.
5. The temperature of the nitrogen bubble in the suppression pool is identical to the temperature of the nitrogen located in the drywell.
6. Following vent clearing, the slug of water located above the top horizontal vent is accelerated in an upward direction while maintaining a constant thickness.
7. The nitrogen in the wetwell is compressed polytropically.
8. To generate a bounding set of PS loads, different polytropic indices are used to generate the PS height and slug velocity results, as well as the wetwell airspace pressurization magnitude. In the calculation of the PS height and slug velocity, a polytropic index of 1.2 is used. Whereas, in the calculation of wetwell airspace pressurization, a polytropic index of 1.4 is used.
9. To ensure a bounding set of PS loads, both high water level (HWL) and low water level (LWL) conditions in the suppression pool are evaluated with a polytropic index of 1.2. LWL conditions with a polytropic index of 1.4 are not needed because peak pressures occur with HWL.
10. The PS velocity is multiplied by a factor of 1.1 to be conservative.
11. To account for a non-uniform rise in the suppression pool (S/P) surface during the swell, the area of suppression pool, which is assumed to be lifted, is 0.8 times the actual suppression pool water surface. This results in higher PS height and velocity.

3.1.3 Analytical Cases

Six test cases are evaluated for pool swell. Table 3-1 lists the conditions for these six cases. These conditions cover the assumptions of Section 3.1.2.

3.2 Pool Boundary Loads

The pool swell results for the ESBWR containment, using the methodology described above, are listed in Table 3-2. The peak values from all six cases are chosen. For the wetwell and bubble pressures, the maximum value occurs with the S/P at HWL and a polytropic constant of 1.4 (Case 1). The maximum pool swell height and surface velocity occurs with the S/P at LWL and a polytropic index of 1.2 (Case 5). The analytical values represent the calculated results while the design values provide margin and are used in subsequent loads evaluations.

During the pool swell phase of LOCA, the wetwell region (the air space and the pool boundaries) is subjected to an internal dynamic pressure loading due to the expanding LOCA air bubble at the vent exits. The maximum wetwell gas-space pressure (P_{WW}) during pool swell, given in Table 3-2, is used in conjunction with the bubble pressure (P_B) loading for structural evaluation of the containment walls. In addition, the wetwell region is simultaneously subjected to external dynamic pressure due to the drywell pressure (P_{DW}) acting on the diaphragm floor and vent wall, as well as the steady reactor building pressure (P_{RB}), which is assumed to be standard atmospheric pressure, acting on the containment wall. Table 3-2 also lists the key drywell-to-wetwell pressures during pool swell. The spatial distributions of the pressure loading conditions are shown in Figure 3-1 for use in structural evaluation. The dynamic pressure loading condition on the inside of the wetwell region acts during the pool swell phase only.

3.3 Structural Impact and Drag Loads Above the Pool Surface

Any structure or component located above the initial pool surface and below the maximum PS height is subject to a water impact load and a dissipative drag load.

3.3.1 Impact Load

The impact load is calculated from the following equation:

$$P(t) = P_{max} [(1-\cos(2\pi t/T))/2] \qquad (3-1)$$

where

$P(t)$ = Pressure acting on the projected area of the structure.
P_{max} = Temporal maximum of the pressure acting on the projected area of the structure.
t = Time.
T = Duration of the impact.

For both cylindrical and flat structures, the maximum pressure P_{max} and pulse duration T are determined as follows:

$$I_P = 1/g_c \cdot M_h V/A_v \qquad (3\text{-}2)$$

where

I_P = Impulse per unit area.
g_c = Conversion constant.
M_h = Hydrodynamic mass of the structure.
V = PS velocity at the structure elevation.
A_v = Projected area of the structure in the vertical direction.

The pulse duration is obtained from the following:

T = Duration of the impact.
= 0.0463D/V, for a cylindrical projected structure.
= 0.011W/V, for a flat projected structure.
[If V < 2.13 m/s for a flat projected structure, then set V = 2.13 m/s.]
D = Diameter of the cylindrical projected structure.
W = Width of the flat projected structure.
(Note that W and D must be specified in meters if V is specified in meters/second.)

The value of P_{max} is obtained using the following equation:

$$P_{max} = 2I_P/T$$

For both cylindrical and flat structures, a margin of 35% is added to the P_{max} values (as specified above) to obtain conservative design loads.

3.3.2 Drag Load

Following the initial impact load, a standard drag load acts on the structure. This drag load is calculated from the following equation:

$$P_D = C_D \rho V^2/2g_c + \rho a V_A/A_v g_c \qquad (3\text{-}2)$$

where

P_D = Drag pressure acting on the projected area of the structure.
C_D = Drag coefficient for the structure.
ρ = Density of the suppression pool water.
V = PS velocity at the structure elevation.
A_v = Projected area of the structure in the vertical direction.
g_c = Conversion constant.

a   = PS acceleration at the structure height.
V_A = Acceleration drag volume.

The drag coefficient C_D is defined in Table 3-3. The hydrodynamic mass M_h and acceleration drag volume V_A are defined in Table 3-4. Values obtained by suitable alternate calculations may also be utilized.

3.3.3   Froth Impact and Drag Loads

Upon reaching the maximum pool swell height, the air bubbles that drive the water slug penetrates through the surface, resulting in bubble breakthrough leading to froth formation. This froth impacts structures located above the maximum bulk swell height. The froth created after breakthrough experiences gravity-induced phase separation and falls back toward the pool bottom. During this fallback, structures are subjected to fallback drag loads.

Structures located at elevations up to 3.3m above the peak pool swell height are subjected to froth impact loading. This froth swell height is the same as that defined for Mark III containment design and was also used in the ABWR design. This is considered to be a conservative value for the ESBWR containment design. Because of substantially smaller wetwell gas space volume (about 1/6th of the Mark III design), the ESBWR containment is expected to experience a froth swell height and velocity substantially lower than that in Mark III design. The wetwell gas space is compressed by the rising liquid slug during pool swell, and the resulting increase in the wetwell gas space pressure would decelerate the liquid slug before the bubble break-through process begins.

The load calculation methodology for defining the froth load is based on USNRC approved methodology in NUREG-0978 (Reference 16). The froth impact load is a triangular pressure pulse with a peak amplitude that varies based on the shape and distance the object is above the suppression pool. The NRC acceptance criterion calls for a pulse duration that would maximize the dynamic loading factor (DLF) for the structure impacted by the froth. This implies that a range of pulse durations must be considered to ensure that the maximum DFL is identified.

Figure 3-10 of NUREG-0978 describes the NRC acceptance criteria for the froth impact load for the Mark III design. The initial height corresponds to the peak pool swell height for Mark III. Figure 3-4 of this report is a reproduction of the NRC acceptance criteria from that NUREG-0978 figure and defines the froth impact pressure for ESBWR.

Concurrent to the duration of the froth impact, the diaphragm floor at the top of the wetwell experiences a downward pressure caused by the drywell pressure exceeding the wetwell pressure. That downward pressure is at least 88 kPad and acts opposite to the upward pressure

caused by froth impact to the bottom of the diaphragm floor or any object below the diaphragm floor and attached to it.

As the drywell air flow rate through the horizontal vent system decreases and the air/water suppression pool mixture experiences gravity-induced phase separation, pool upward movement stops and the "fallback" process starts. During this process, structures between the bottom vent and the peak froth elevation can experience loads as the mixture of air and water fall past the structure. The load calculation methodology for the fallback load definition is based on the USNRC approved methodology in NUREG-0978 (Reference 8). That is, the load on all those structures is based on the standard drag resulting from solid water flowing at 10.7 m/sec which is the terminal velocity resulting from a 6.1m free fall. Because the ESBWR peak pool swell height is less than the basis for this condition, this free fall velocity is conservative.

3.4   Vacuum Breaker Load Due to Wetwell Nitrogen Compression

The potential for rapid actuation of the wetwell-to-drywell vacuum breakers exists when the wetwell airspace compression exceeds the pressurization of the drywell. However, in the design of the ESBWR this potential load is not postulated due to the wetwell airspace pressure always remaining lower than the drywell pressure during the PS phase of the transient. Figures 3-2 and 3-3 show the postulated drywell and wetwell pressures for the six cases analyzed. Therefore, this load does not exist during the PS phase of the LOCA in the ESBWR.

3.5   Loads on Diaphragm Floor

Rapid pressurization of the wetwell airspace during the pool swell transient has a potential for upward differential pressure loading on the diaphragm floor. Results from the pool swell analytical model, however, showed that wetwell airspace pressure did not exceed the drywell pressure during the pool swell transient. Hence, it is concluded that the diaphragm floor will not be subjected to an upward differential pressure loading. The diaphragm floor will be subjected to only downward pressure differential loading (Table 3-2), during the pool swell phase.

Table 3-1. Pool Swell Cases

Parameter	Case 1	Case 2	Case 3	Case 4	Case 5	Case 6
S/P Area (%)	100	80	80	100	80	100
Polytropic Constant	1.4	1.4	1.2	1.2	1.2	1.2
S/P Water Level	HWL	HWL	HWL	HWL	LWL	LWL

Table 3-2. Pool Swell Results

Description	Calculated Value	Design Value	Units
Maximum Nitrogen Bubble Pressure (P_B) [a]	245	350	kPa
Maximum Pool Swell Velocity [b, c]	5	6	m/s
Maximum Wetwell Gas Space Pressure (P_{WW}) [a]	237	350	kPa
Maximum Pool Swell Height [b]	4.1	4.5	m
Drywell-to-Wetwell Differential Pressure ($P_{DW} - P_{WW}$) • Maximum [b] • At Peak Wetwell Gas Space Pressure [a]	120 9	241 64	kPa(d)

[a] Polytropic index = 1.4
[b] Polytropic index = 1.2
[c] Reflects conservative multiplier of 1.1

Table 3-3. Standard Drag Coefficients for Various Objects
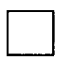
Body Shape			C_D	Reynolds Number	L/d
Circular cylinder	↔	◯	0.63	10^5	1
			0.74	10^5	5
			0.90	10^5	20
			1.20	10^5	∞
			0.35	$> 5 \times 10^5$	5
			0.33	$> 5 \times 10^5$	∞
Elliptical cylinder	↔	◯ 2:1	0.0	4×10^4	∞
			0.46	10^6	∞
	↔	◯ 4:1	0.32	2.5×10^4 to 10^5	∞
			0.29	2.5×10^4	∞
	↔	◯ 8:1	0.20	2×10^5	∞
Square cylinder	↔	▢	2.0	3.5×10^4	∞
	↔	◇	1.6	10^4 to 10^5	∞
Triangular cylinders	↔	▷ 120°	2.0	10^4	∞
	↔	◁	1.72	10^4	∞
	↔	▷ 90°	2.15	10^4	∞
	↔	◁	1.60	10^4	∞
	↔	▷ 60°	2.20	10^4	∞
	↔	◁	1.39	10^4	∞
	↔	▷ 30°	1.8	10^5	∞
	↔	◁	1.0	10^5	∞
Semi-tubular	↔	⊃	2.3	4×10^4	∞
	↔	⊂	1.12	4×10^4	∞
Circular disk, normal to flow	↔		1.12	$> 10^3$	0
			1.12	$> 10^3$	0
Circular cylinder parallel to flow	↔		0.91	$> 10^3$	1
			0.87	$> 10^3$	4
			0.99	$> 10^3$	7

Table 3-3. Standard Drag Coefficients for Various Objects

Body Shape	C_D	Reynolds Number	L/d
Rectangular flat plate, normal to flow	1.10	$\geq 10^3$	1
	1.20	$> 10^3$	5
	1.50	$> 10^3$	20
	2.00	$> 10^3$	∞

L = Length
d = Maximum width of object measured normal to flow direction

Table 3-4. Hydrodynamic Mass and Acceleration Drag Volumes for Two-Dimensional Structural Components and Three-Dimensional Structures
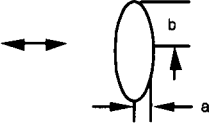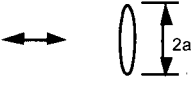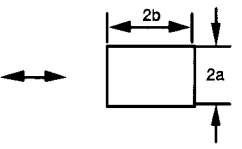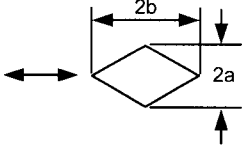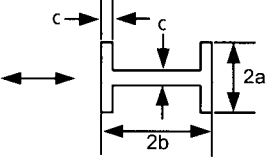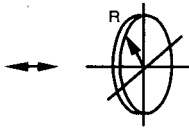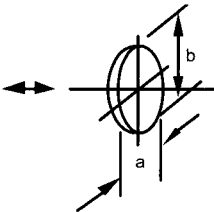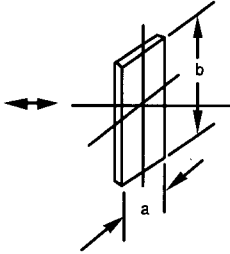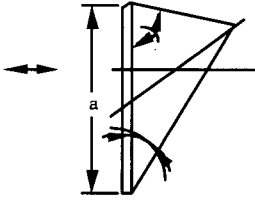
Body	Section Through Body and Uniform Flow Direction	Hydrodynamic Mass (M_h)	Acceleration Drag Volume (V_A)
Circle		$\rho\pi R^2 L$	$2\pi R^2 L$
Ellipse		$\rho\pi a^2 L$	$\pi a(a+b)L$
Ellipse		$\rho\pi b^2 L$	$\pi b(a+b)L$
Plate		$\rho\pi a^2 L$	$\pi a^2 L$
Rectangular		$\begin{array}{ll} a/b & \\ \infty & \rho\pi a^2 L \\ 10 & 1.14\rho\pi a^2 L \\ 5 & 1.21\rho\pi a^2 L \\ 2 & 1.36\rho\pi a^2 L \\ 1 & 1.51\rho\pi a^2 L \\ 1/2 & 1.70\rho\pi a^2 L \\ 1/5 & 1.98\rho\pi a^2 L \\ 1/10 & 2.23\rho\pi a^2 L \end{array}$	$aL(4b+\pi a)$ $aL(4b+1.14\pi a)$ $aL(4b+1.21\pi a)$ $aL(4b+1.36\pi a)$ $aL(4b+1.51\pi a)$ $aL(4b+1.70\pi a)$ $aL(4b+1.98\pi a)$ $aL(4b+2.23\pi a)$
Diamond		$\begin{array}{ll} a/b & \\ 2 & 0.85\rho\pi a^2 L \\ 1 & 0.76\rho\pi a^2 L \\ 1/2 & 0.67\rho\pi a^2 L \\ 1/5 & 0.61\rho\pi a^2 L \end{array}$	$aL(2b+0.85\pi a)$ $aL(2b+0.76\pi a)$ $aL(2b+0.67\pi a)$ $aL(2b+0.61\pi a)$
I-Beam		$a/c=2.6,\ b/c=3.6$ $2.11\rho\pi a^2 L$	$[2.11\pi a^2 + 2c(2a+b-c)]L$

Table 3-4. Hydrodynamic Mass and Acceleration Drag Volumes for Two-Dimensional Structural Components and Three-Dimensional Structures

Body	Section Through Body and Uniform Flow Direction	Hydrodynamic Mass (M_h)	Acceleration Drag Volume (V_A)
Circular Disk		$\frac{8}{3}\rho R^3$	$\frac{8}{3}R^3$
Elliptical Disk		b/a ∞ $\rho\pi/6ba^2$ 3 $0.9\rho\pi/6ba^2$ 2 $0.826\rho\pi/6ba^2$ 1.5 $0.748\rho\pi/6ba^2$ 1.0 $0.637\rho\pi/6ba^2$	$\pi/6ba^2$ $0.9\pi/6ba^2$ $0.826\pi/6ba^2$ $0.748\pi/6ba^2$ $0.637\pi/6ba^2$
Rectangular Plate		b/a 1 $0.478\rho\pi/4a^2b$ 1.5 $0.680\rho\pi/4a^2b$ 2 $0.840\rho\pi/4a^2b$ 2.5 $0.953\rho\pi/4a^2b$ 3 $\rho\pi/4a^2b$ ∞ $\rho\pi/4a^2b$	$0.478\pi/4a^2b$ $0.680\pi/4a^2b$ $0.840\pi/4a^2b$ $0.953\pi/4a^2b$ $\pi/4a^2b$ $\pi/4a^2b$
Triangular Plate		$\rho a^3 \dfrac{(\tan\theta)^{3/2}}{3\pi}$	$a^3 \dfrac{(\tan\theta)^{3/2}}{3\pi}$
Sphere		$\rho\frac{2}{3}\pi R^3$	$2\pi R^3$
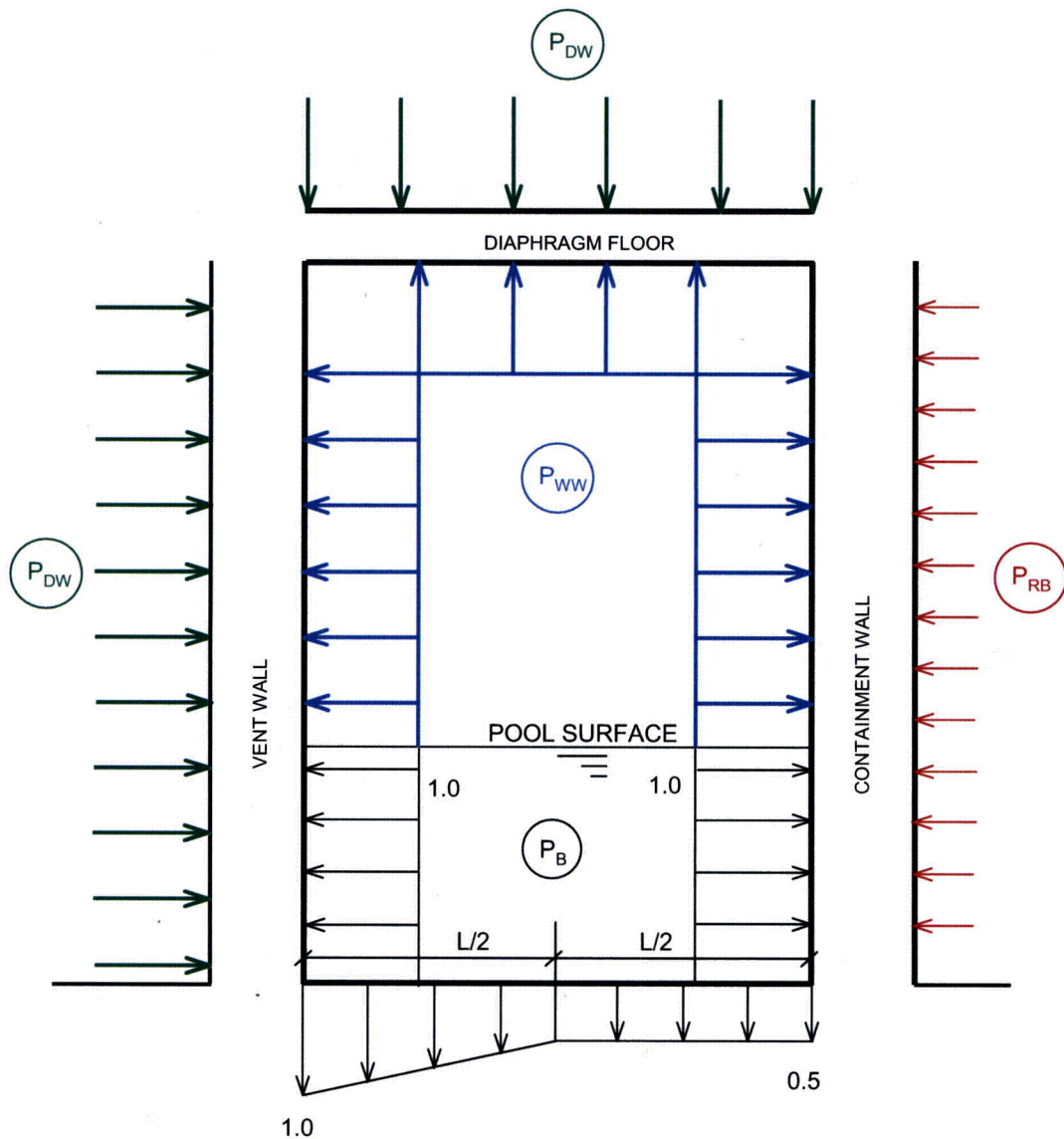
Figure 3-1. Pool Swell Normalized Pressure Spatial Distributions for Bubble (P_B), Wetwell (P_{WW}), Drywell (P_{DW}), and Reactor Building (P_{RB}) Pressures

[[

]]

Figure 3-2. Containment Pressure Response During Pool Swell MSLB Event - HWL

[[   ]]

Figure 3-3. Containment Pressure Response During Pool Swell MSLB Event - LWL
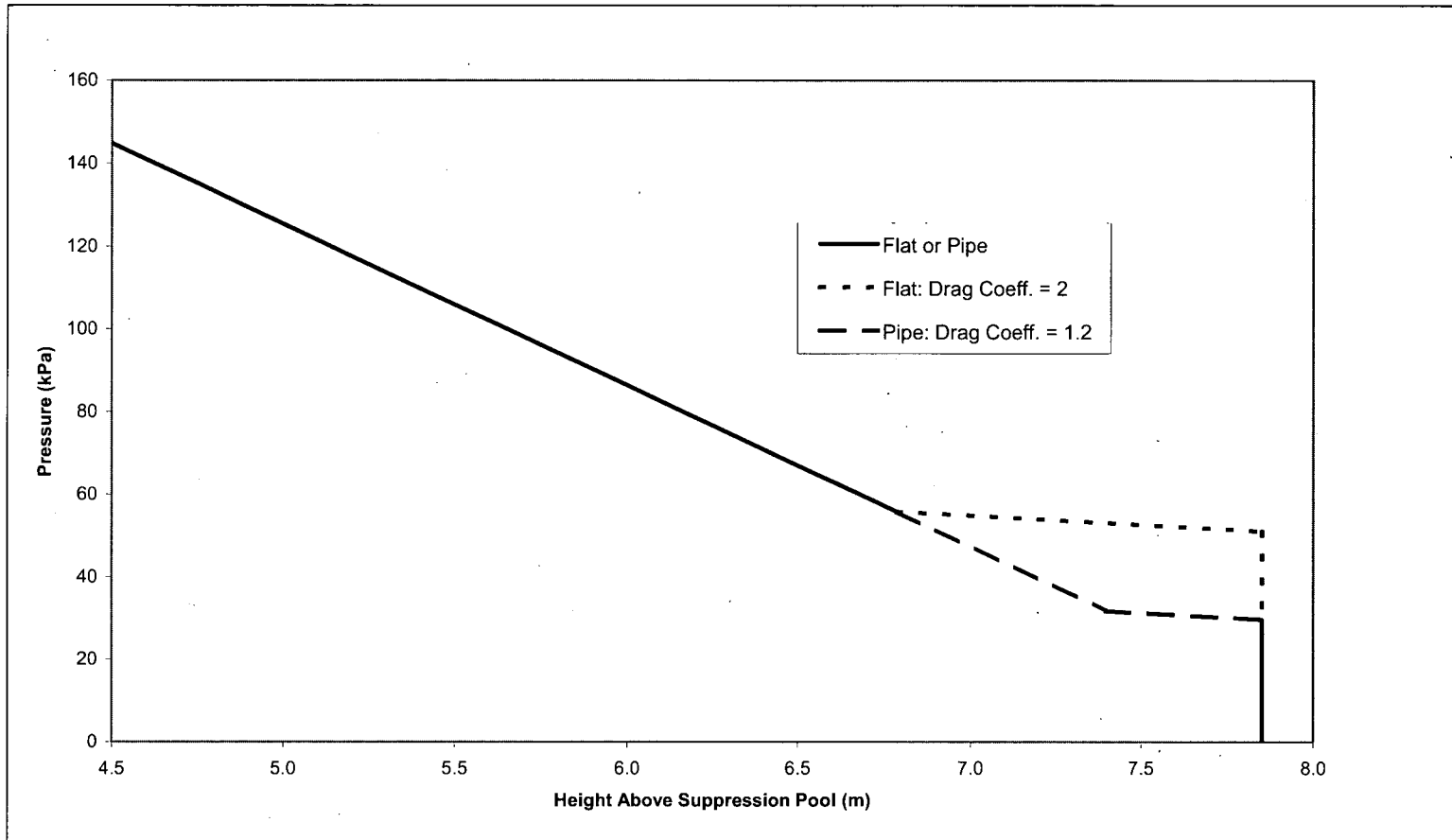
Figure 3-4. Pool Swell Froth Impact

4.0   CONDENSATION OSCILLATION LOADS

The term Condensation Oscillation (CO) is used to represent a hydrodynamic/steam condensation phenomenon associated with a LOCA.   During the initial phase of the DBA, pressurized drywell nitrogen is purged into the wetwell.   Steam condensation then begins after the vents are cleared of water and the drywell nitrogen has been carried over into the wetwell. The CO phase is vibratory in nature and induces a bulk water motion.   CO occurs typically at higher mass fluxes compared to chugging (Section 5.0).   During this period of high steam flow rate, the liquid-steam interface is located inside the wetwell, just beyond the horizontal vent exit. Experiments for Mark III and ABWR indicate that the interface oscillates at frequencies ranging primarily from 2 to 10 Hz, thereby producing a cyclical loading on all submerged containment structures and boundaries due to acoustic propagation of the source pressure.   The CO phase persists until the mass flux falls below the so-called chugging threshold level.   At this point the relatively regular CO loads changes to the more stochastic, impulsive chugging phenomenon.

A CO load is defined for the ESBWR and used in evaluation of affected structures. Figure 4-1 gives a side view comparison of the main vent and suppression pool between the ESBWR and the ABWR.   Because of the similarity between the ESBWR and ABWR containments, the ESBWR CO load is defined based on the ABWR CO load definition.

Section 4.0 provides a description of the ABWR CO load definition, including the ABWR test program, the basis for application to the ESBWR, and any adjustments made to the ABWR CO load definition for application to the ESBWR.

4.1   ABWR Horizontal Vent Test Program

LOCA loads with the horizontal vent system design have been well characterized during the Mark III Confirmatory Test Program.   More than 200 tests have been performed to determine horizontal vent system performance and associated LOCA loads.   However, all of these tests have utilized the relatively lower containment pressure characteristics of the Mark III containment system.   Because of some thermodynamic and geometrical differences between the ABWR and Mark III designs, it was anticipated that condensation oscillation (CO) and chugging (CH) loads might differ from prior (Mark III) testing in horizontal-vent facilities.   These included the following

1. Increased ABWR wetwell airspace pressure, and hence subcooling,
2. The presence of a lower drywell,
3. The smaller number of vents (30 in ABWR vs. 120 in Mark III),
4. Extension of the vents in the pool,

5. Vent submergence, and

6. Suppression pool width.

Considering the existence of the above thermodynamic and geometrical differences, a test program was conducted to confirm the CO and CH loads, which would occur in the event of a LOCA in an ABWR plant. The ABWR Horizontal Vent Test (HVT) program, test data and interpretation of test data are documented in Reference 4.

The test program consisted of 24 simulated blowdowns in a test facility representing the horizontal-vent ABWR design. The tests were divided into two parts utilizing sub-scale (SS) and partial full-scale (FS*) test configurations. Figure 4-2 gives the side view of the SS test configuration. Figure 4-3 gives a top view of the HVT facility along with the equivalent sector for the ESBWR and ABWR.

The SS facility had all linear dimensions reduced by a factor of 2.5 from prototypical dimensions. Thirteen SS tests were performed primarily for the purpose of obtaining CO data. A full-scale vertical and horizontal-vent configuration was installed for the FS* tests. The upper drywell was enlarged but not to prototypical dimensions. Eleven FS* tests were performed primarily for the purpose of obtaining CH data. The test matrix for the 24 blowdowns included variations in pool temperature, break size, wetwell backpressure, and type of break (steam or liquid). The test facility was equipped adequately with the data sensors to obtain necessary data for understanding the phenomena and establishing a database for defining CO and CH loads for the ABWR containment. In addition to the geometrical considerations, the facility was designed to minimize the potential for fluid-structure interaction (FSI). Measurements were taken at seven locations on the wetted suppression pool boundary to record dynamic pressure oscillations. Structural instrumentation (strain gauges and accelerometers on the basemat, pedestal, and containment walls) was used to confirm that FSI effects were minimal. Pressure transducers in the vertical and horizontal vents recorded dynamic loads on the vent system.

4.1.1 Description of CO Database

A detailed description, evaluation and discussion of CO data are given in Reference 4.

The test program consisted of a total of 13 simulated blowdowns in a sub-scaled test facility representing a one-cell (36°) sector of the horizontal vent design, which included a signal vertical/horizontal vent module. The sub-scaled (SS) test facility was geometrically (all linear dimensions scaled by a factor of 2.5) similar to the prototypical design, and the single vertical/horizontal vent module included all three horizontal vents. In these tests, full-scale thermodynamic conditions were employed. This approach is based on the belief that condensation phenomena at the vent exit are mainly governed by the thermodynamic properties

of the liquid and vapor phases. In accordance with this scaling procedure, measured pressure amplitudes are equal to full-scale values at geometrically similar locations, whereas measured frequencies are 2.5 times higher than the corresponding full-scale frequencies. The technical basis for using this scaling approach was based on extensive review and evaluation of the available literature on CO scaling and scaled tests performed for Mark II and Mark III containments, as well as general consensus of technical experts in this field. The CO scaling studies, which have been performed independently by various technical experts, show that for tests in a geometrically scaled facility with full-scale thermodynamic conditions, the measured pressure amplitudes are the same as full-scale values at geometrically similar locations, and measured pressure frequencies are the scale factor times higher than the corresponding full-scale frequencies.

Therefore, CO frequencies for the full-scale prototypical design are obtained by scaling the frequencies measured in SS tests by a factor of 2.5. A similar technique is applicable to scaling adjustment in frequency for obtaining full-scale values. Thus, this scaling procedure made it possible to use the measured SS data (pressure time history) directly for load definition purpose after the time scale is compressed by a factor of 2.5.

Out of the 13 SS tests, the tests recommended for definition of the CO load are SST-1, 2, 3, 9, 11, and 12. These six tests were run at prototypical conditions. Of the remaining tests, SST-4, 5, 6, 7, 8, and 14 were run with a pre-purged vent system, and SST-10 was run with the lower drywell blocked off. These tests are valuable for understanding CO phenomena and the effects of system variables, but they are not considered to be an appropriate basis for the CO load definition.

4.1.2 Evaluation of CO Database

Each of the CO load definition tests showed significant frequency peaks at 5 and 9 Hz. The 9 Hz frequency is dominant early in the CO period and the 5 Hz frequency is dominant late in the CO period.

Further examination of the data shows that, in general, the largest amplitude loads occurred at a transducer located on the basemat, near the pedestal wall. The highest amplitude CO loads occurred during the first 30 seconds of tests SST-1 and 2 (large liquid breaks at elevated pool temperature). Examination of the Power Spectral Density (PSD) data showed that the envelope PSD of the pressure from a 12-second segment in SST-1 and an 18-second segment in SST-2 matched the envelope PSD of the pressure from the six-test database.

4.2 Source Load Approach

The CO load, termed as "Source Load Approach," is used to develop a source load. The source load is a series of pulses, which simulate the oscillation of the steam/water interface at the horizontal vent exits. In this approach the CO source load would be applied to a coupled fluid-structure model of the prototypical containment as an excitation of the steam/water interface at the exits of the horizontal vents. It is the oscillatory motion of the steam/water interface which produces the characteristic oscillatory pressure loading on the wall. With a source load, it is possible to account for the spatial distribution of the load and the variation of pool and vent fluid properties in a natural way. This approach avoids the problem of artificial resonant amplification at the system frequencies.

Figure 4-4 describes the CO source load methodology. In order to develop a technically justified source loading function, the methodology includes the following elements:

1. A comprehensive test database
2. A coupled steam-water-structure interaction model of the test facility from which the data were obtained
3. A procedure to develop a "test source" loading configuration
4. A criteria to evaluate the test source loading configuration and test facility model
5. A procedure to scale up the test source to a full-scale design source for the prototypical containment system
6. A full-scale coupled steam-water-structure interaction model of the prototypical containment system
7. A criteria to evaluate the design source loading condition for the prototypical containment system
8. Calculation of CO design (wall pressure) from the prototypical analysis using the design source

Criteria for CO Source Load

An acceptance criterion is specified in order to provide a basis for judging the acceptability of the source loading function with respect to prediction of wall pressure loadings and their frequency contents. The criteria include the following elements:

1. Wall pressure histories for the SS test facility produced by the test source match with the pressures measured in the SS test facility.
2. Frequency content of the predicted pressure histories, as defined by a power spectral density (PSD) and by an amplitude response spectrum, matches with the data obtained from the SS test facility.
3. Spatial distribution of the root mean square (RMS) of the predicted loading matches with the data measured from the SS test facility.

4. Wall pressures predicted by the design source for the prototypical ABWR match with the pressures measured in the SS test facility at geometrically similar locations. Note, this is required by the CO scaling laws (Reference 5)

4.3   Basis for ESBWR Load Definition

The ESBWR CO load definition utilizes the ABWR CO load definition. Adjustments, as necessary are made to the ABWR CO load definition for ESBWR application. The adjustments are determined from a review of predicted thermal-hydraulic conditions during CO in the ESBWR, a review of the ESBWR and ABWR geometry, and a review of test data from the ABWR Horizontal Vent Tests (HVT) sub-scale tests (SST) and tests from the Mark III containment Pressure Suppression Test Facility (PSTF) tests.

4.3.1   Review of ABWR and ESBWR Containment Geometry

The ESBWR and ABWR have a similar containment vent system design. Key differences between the ESBWR and ABWR are shown in Table 4-1.

In the ESBWR and ABWR designs, the drywell and suppression pool are connected by a set of circular vertical vents which are equally spaced around the containment. Each vertical vent contains a set of three horizontal vents, which connect the vertical vent to the suppression pool. The horizontal vent diameter and vertical vent diameters are the same for the ABWR and ESBWR designs. The distance from the suppression pool floor to the bottom horizontal vent and the distance between the bottom, middle and top horizontal vents are the same for the two designs. The distance the horizontal vents extend into the suppression pool is the same for the ESBWR and ABWR.

The containment design differences (Table 4-1), which do exist between the ABWR and ESBWR, will tend to produce lower CO pressure amplitudes for the ESBWR. These key differences include

1. A lower pool depth and vent submergence for the ESBWR
2. Two additional vertical vents for the ESBWR
3. A longer distance between the horizontal vent exit and the outer containment wall

The ABWR contains 10 equally spaced vertical vents, at 36° intervals, whereas the ESBWR contains 12 vertical vents equally spaced at 30° intervals. However, the ESBWR containment size is larger than in the ABWR design. Consequently, the ESBWR has a pool surface area per vent which is approximately 30% greater than the value for the ABWR. This means that pressure disturbances in the suppression pool induced by CO are dispersed over a wider area before impacting pool-wall boundary surfaces resulting in lower wall pressures. The larger pool surface area per vent for the ESBWR will result in lower CO wall pressures. The smaller pool

depth and associated lower vent submergence for the ESBWR increases the pressure attenuation to the pool surface. This produces lower CO wall pressure amplitudes at all submerged boundaries. The longer distance from the vent exit to the outer containment wall increases the pressure attenuation to the outer containment wall, which further reduces the outer containment wall pressures.

4.3.2   Review of Thermal-Hydraulic Conditions

Key parameters, which can affect the CO load, include the vent steam mass flux and pool temperature. The ABWR HVT tests show that CO amplitudes increase significantly with increased vent steam mass flux and pool temperature. The HVT test data also indicate that higher containment pressures tend to reduce CO pressure amplitudes. This is attributed to the higher subcooling associated with the higher containment pressure.

HVT test SST-1 results are used to define the CO load for ABWR. Figure 4-5 shows the measured main vent steam mass flux for that HVT test as a function of the suppression pool temperature along with the predicted values for the ESBWR MSLB and FWLB. The predicted steam mass fluxes for the ESBWR MSLB and FWLB events are shown to be well below the measured test values for the load definition test. In addition, Figure 4-6 shows that the SST-1 test values of vent steam mass flux as a function of the exit subcooling are also bounding relative to ESBWR predictions for the MSLB and FWLB. Consequently, CO pressure amplitudes associated with predicted ESBWR thermal-hydraulic conditions are bounded by the CO pressures determined from the ABWR HVT CO load definition tests.

4.3.3   Frequency Content Evaluation

An additional consideration for the CO load is the CO frequency. The thermal hydraulic conditions at the vent exit (and vent diameter) mainly govern the condensation processes at the vent exit which establish the CO "driver frequency." This is the basic premise of the scaling laws used to apply the sub-scale data to full-scale. However, the vent system geometry can affect the vent acoustic modal frequencies, which may influence the CO frequency also.

Thermal-hydraulic Conditions

The key thermal-hydraulic parameters that affect the vent exit frequency include mass flow rate, nitrogen content and pool temperature. Additionally, the CO frequency is found to be directly proportional to the vent exit diameter. However, the vent diameters for the ABWR and ESBWR are the same and therefore do not present a source of frequency content change.

The range of conditions tested in the HVT tests cover the predicted range of thermal-hydraulic conditions for the ESBWR during the CO period. Because the maximum predicted ESBWR

steam mass fluxes are lower, the CO frequencies will be concentrated at the lower range and covered by the range of frequencies associated with the HVT SST CO data used to define the ABWR CO load.

Containment Vent Geometry

Differences in the ESBWR vent system geometry relative to the ABWR design, which can affect the vent acoustic modes, include the difference in the vertical vent length, and the difference in the lower drywell configuration. The ESBWR vertical vent length is smaller than the ABWR vent length. Additionally, in the ABWR containment design, there is a direct connection between the lower drywell and the vertical vent. For the ESBWR containment design this connection between the lower drywell and vertical vent is not present. Instead the lower drywell connects to the upper drywell through flow paths between the bottom of the upper drywell and top of the lower drywell.

To evaluate the effect of these differences, the HVT CO test data are reviewed. Additionally, data from the Mark III Containment PSTF tests are also reviewed. The purpose of the review is to establish the controlling influence on CO frequency.

Analytical studies of CO for Mark III containments are documented in Reference 5 and in GESSAR II (Reference 6). These studies have determined that high steam mass flux and low pool temperature conditions produce high CO vent exit driving frequencies while low steam mass flux and high suppression pool temperatures produce low frequencies. This trend is supported by the Mark III PSTF CO test data (Reference 7).

As previously described, the load definition CO data show dominant peaks at 5 Hz and at 9 Hz. The 9 Hz peak is dominant early in the CO period of the tests, whereas the 5 Hz peak is dominant late in the CO period. A high steam mass flux and low pool temperature characterize these tests early in the CO period and low steam mass flux and high pool temperature late in the CO period. CO data from a smaller sized liquid break and a steam break, both with relative low steam mass fluxes, show only one dominant peak near 5 and 6 Hz.

These HVT SST test results are consistent with CO frequencies, which are controlled by the vent exit thermal-hydraulic conditions.

It had been postulated in Reference 4 that the lower 5 Hz peak seen in the HVT tests, which occur with lower mass fluxes, may be tuned into the vent acoustic modal frequency associated with the lower drywell connection to the vertical vent. The results of a test, which did not model the connection between the lower drywell to the vertical vent, are reviewed to examine this possibility. The CO data for this test show a dominant CO wall pressure frequency near 6 Hz and a small secondary wall pressure frequency peak near 13 Hz. The presence of a dominant

PSD frequency peak near 6 Hz without the lower drywell modeled, indicates that vent acoustic modes associated with the connection to the lower drywell did not have a significant influence on this CO frequency.

The Mark III PSTF CO data are also reviewed. The Mark III $1/\sqrt{3}$ scale PSTF CO test data show that dominant frequencies in sub-scale when scaled up to full-scale are near 3 Hz, which is within the range of full-scale dominant frequencies of $2 - 4$ Hz determined for the ABWR. The trends in the CO frequency with test conditions shown for the Mark III $1/\sqrt{3}$ scale PSTF tests are also similar to the ABWR HVT test results. As with the HVT CO tests, higher Mark III PSTF CO frequencies are observed at high mass flux and low pool temperature conditions and lower CO frequencies are observed at low mass flux and high pool temperature.

Considering that the Mark III PSTF and HVT test facilities have expectedly different vent acoustic modes, the fact that the Mark III (PSTF) and ABWR (HVT) produce similar dominant CO frequencies supports the hypothesis that the ABWR (and ESBWR) CO frequency is mainly governed by the vent exit thermal-hydraulic conditions and not the vent acoustic modes.

From this review of ABWR HVT CO test data and Mark III PSTF CO tests data it is determined that, although there may be some contribution of vent acoustic modes, CO frequencies are controlled by vent exit thermal-hydraulic conditions. Therefore, differences in the vent geometry between the ESBWR and ABWR, and associated changes to the vent acoustic modes, would not impact the frequency content of the ABWR CO load definition when applied to the ESBWR.

4.4 Application of the ABWR CO Load to the ESBWR

For the design evaluation of the containment structure, the pool boundary pressure load is obtained from an analysis of single-vent model of the ABWR prototypical design. The pool boundary pressure load obtained from the ABWR model analysis is applied over the full model of the ESBWR configuration. This CO loading specification implies that all vertical vents are in phase (i.e., no credit for phasing among vents), which is considered to be a conservative load definition approach.

For analysis of the structure, the pool boundary load is specified as a pressure time history. A total of four CO pool boundary pressure time histories are generated using the prototypical ABWR single vent model representing different observed periods of CO behavior. A fifth CO history is added for application to the ESBWR by compressing the time scale of the time history with highest frequency content. The time scale compression factor corresponds to the ratio of the ESBWR-to-ABWR vertical vent distance between the drywell entrance and top vent entrance. Although vent acoustic modes do not control CO frequency, this additional time history is added to account any possible influence of vent acoustic modes on the CO frequency.

For added conservatism with ESBWR applications, a multiplication factor of 1.2 is also applied to the ABWR CO wall pressure history. Figure 4-7 shows the spatial distribution of CO loads around the ESBWR submerged pool boundary normalized by the CO pressure time history.

4.5   Local Condensation Oscillation Loads

In the horizontal vent confirmatory tests, a CO load with large positive pressure amplitude and short duration was observed on the bottom liner near the bottom vent exit. These pressure spikes were not observed outside a radius of two vent diameters from the bottom vent exit centerline.

Therefore, an additional CO load (Figure 4-8) is considered in the design of the suppression pool floor/liner and submerged structures located within 2 vent diameters of each horizontal vent. The amplitude of this load represents the highest pressure measured during the HVT-SS tests. Structure responses from this local CO load are combined with responses from the pool boundary load specified in Section 4.4 as absolute sum.

Table 4-1. Key Differences Between ESBWR and ABWR Containments

Parameter	ESBWR	ABWR
Number of Vertical Vents	12	10
Suppression Pool Angular Sector Per Vertical Vent (deg)	30	36
Pool Depth (m)	5.5	7.1
Top Vent Submergence (m)	2.0	3.6
Distance from Vent Exit to Outer Containment Wall (m)	9.0	6.85
Pool Surface Area per Vent (m^2)	66.6	50.7
Vertical Vent Distance Between Drywell Entrance and Top Vent Entrance (m)	9.35	17.0
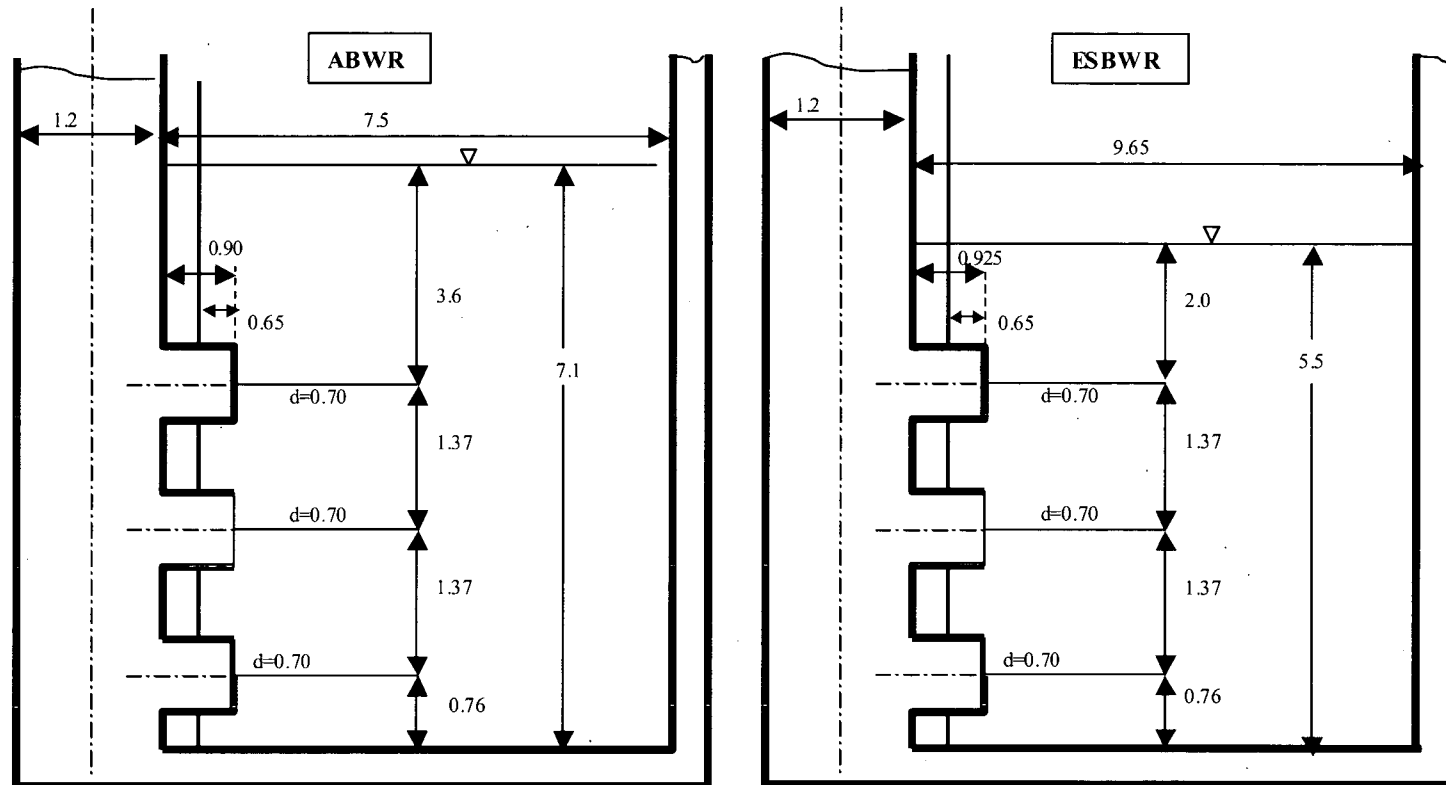
(Dimensions in meters)

Figure 4-1. Side View Comparison ESBWR vs. ABWR

[[   ]]

Figure 4-2. HVT SST Test Facility

[[°   ]]

Figure 4-3. Top View – ESBWR, ABWR and HVT
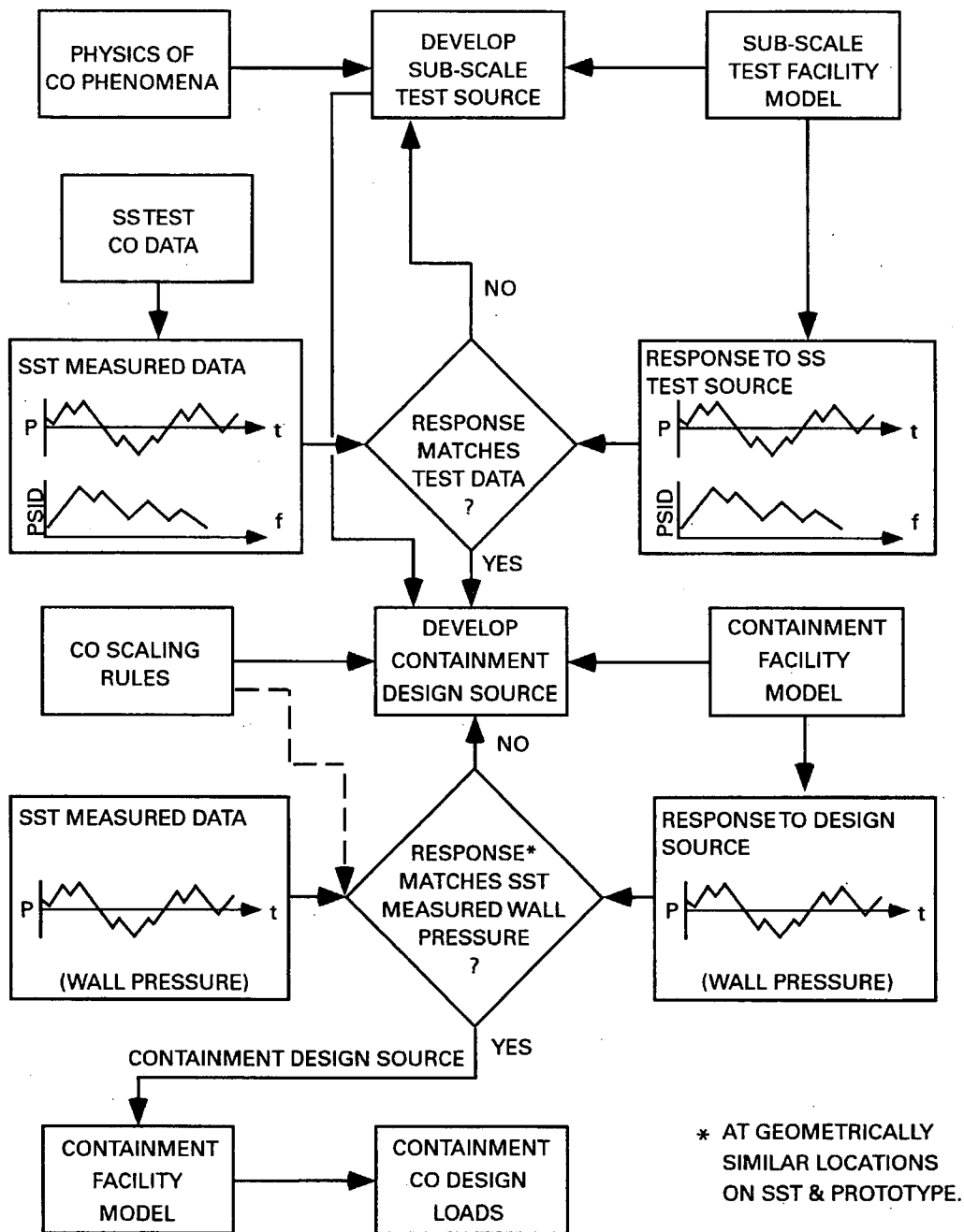
Figure 4-4. Containment CO Source Load Methodology

[[   ]]

Figure 4-5. Main Vent Steam Flux During CO Phase

[[   ]]

Figure 4-6. Main Vent Exit Conditions During CO Phase
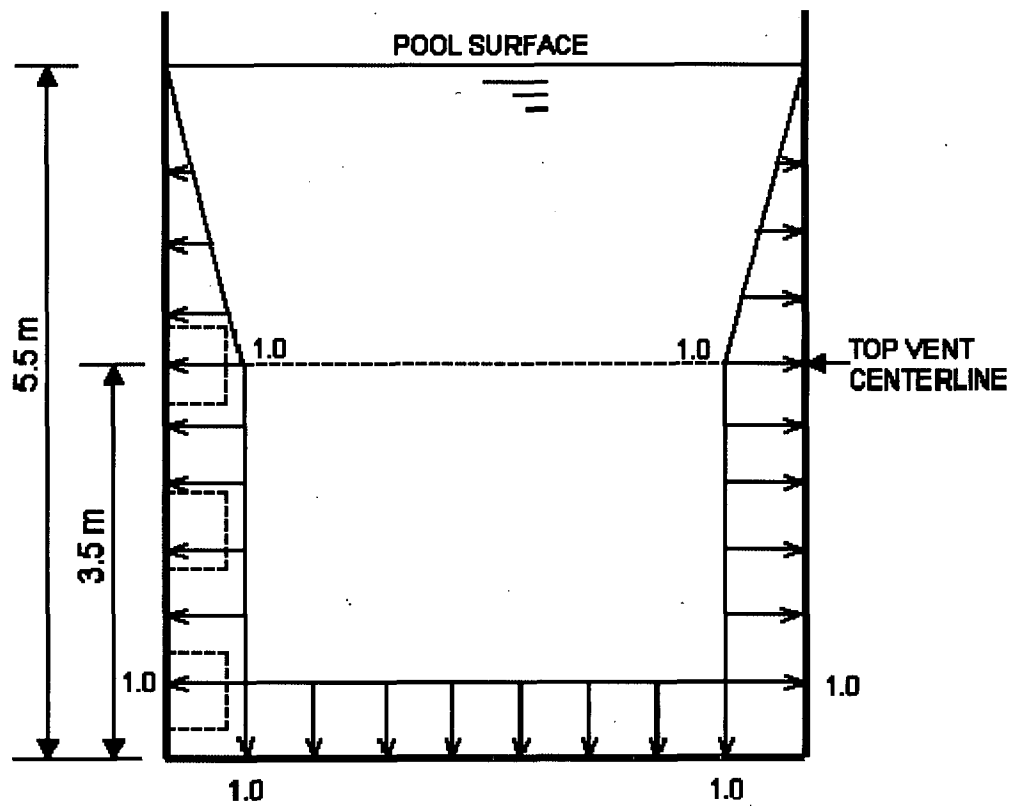
Figure 4-7. Spatial Load Distribution for CO

[[   ]]

Figure 4-8. Local CO Load (Apply 1.2 Multiplier to Amplitude for ESBWR)

5.0   CHUGGING LOADS

Chugging (CH), or unsteady condensation is a design consideration in pressure suppression containment systems using horizontal or vertical vents. It is generally used to represent a hydrodynamic phenomena associated with a LOCA. For the ESBWR design, CH is a manifestation of low horizontal vent steam mass flux. During chugging, rapid steam condensation causes the pool water to re-enter the vents. This is followed by a quiescent period until the steam-water interface is forced out into the pool. Thus, chugging, an intermittent event, is the result of unsteady condensation occurring in the last stages of the blowdown. Consequently, during a LOCA, chugging would typically occur following Condensation Oscillation as described earlier in the report. The exact transition between CO and CH is a function of mass flux and pool temperature.

The dominant pressure response in the suppression pool during CH is characterized by a prechug under-pressure, an impulse (pressure spike), and a post chug oscillation. These are caused by the rapid condensation and subsequent collapse of a steam bubble located either inside or at the exit of one of the horizontal vents. As a result of this sudden collapse, water is allowed to re-enter the vent. After a short (one to five seconds) quiescent period, the pressure in the drywell again forces the steam water interface back out into the suppression pool. When the rate of pressurization can no longer keep up with the rate of condensation, the bubble collapses, and the cycle begins again. Overall, CH can be classified as an intermittent event resulting from the unsteady condensation of steam during the final phases of the drywell blowdown.

Specific tests at the Horizontal Vent Test (HVT) Facility were conducted to obtain chugging data for defining the chugging loads for the ABWR containment system.

As with CO, the ESBWR chugging load is defined based on the ABWR chugging load definition. A description of the ABWR chugging load definition, the basis for application to the ESBWR, and any required adjustments made to the ABWR chugging load definition for application to the ESBWR are described within Section 5.0.

5.1   Description of Chugging Data

Section 4.1 describes the HVT Facility. The test program, test data, and interpretation of test data are documented in Reference 4. The tests were divided into two parts utilizing sub-scale (SS) for CO and partial full-scale (FS*) test configurations for CH. Figure 5-1 gives the side view of the FS* test configuration. Figure 4-3 gives a top view of the HVT facility along with the equivalent sector for the ESBWR and ABWR.

There were 11 tests performed primarily for the purpose of establishing a database for definition of the CH load for a prototypical design evaluation. The HVT facility for the FS* test series was run with a full-scale vertical vent and horizontal vent system and an enlarged upper drywell. The tests were run at prototypical mass flux and pool temperature and with the vent system purged of nitrogen. It is known from previous blowdown testing and observations that presence of nitrogen in the vent reduces CH loads, so running chugging tests at pre-purged conditions is conservative.

5.2   Evaluation of Chugging Data

A detailed description and discussion of chugging data are contained in Reference 4.

As previously described, chugging is characterized by a small under-pressure, followed by a positive pressure pulse, and a decaying ring-out. These phenomena are associated with the initial contraction of the steam bubble, the rapid deceleration of pool water converging on the vent exit, and the excitation of an acoustic standing wave in the pool.

Chugging data from the Reference 4 tests clearly show that the most severe chugging occurs for the steam breaks with an initial cold pool temperature. Both peak over-pressure and Root-Mean-Square pressures decrease significantly as the pool temperature rises. In general, the data support the understanding (observed from prior tests) that chugging has some dependence on system parameters, such as mass flux and pool temperature, along with a substantial degree of randomness.

5.3   Chugging Load Definition

Figure 5-2 shows various elements of the source load methodology for defining the chugging load on the pool boundary. The database consisted of 11 tests conducted in the HVT facility with the full-scale vent system. From this database, key chugs were selected which serve as criteria for the development of the source load. The key-chug approach was used successfully for the definition of the chugging load for Mark II containment design (Reference 8).

Key chug selection was determined by requiring that the PSD envelope of the selected key chugs matches the PSD envelope of the FS* chugging database. The criterion for a technically justifiable chug design source is that the design source load, when applied to an analytical model of the HVT facility, produces a wall pressure which matches the selected data and a PSD envelope which envelops the PSD envelope of the selected data.

Eight different chugging design sources, represented by a single pulse acting at the exit of top vent in a full-scale model, were defined. The design sources were determined by imposing a

requirement that the PSD envelope generated by these design sources bounds the PSD envelope from the selected chugging data.

5.4   Basis for ESBWR Chugging Load Definition

The ESBWR chugging load definition is based on the ABWR definition. Adjustments to the ABWR definition for ESBWR application are determined from a review of expected conditions during chugging in the ESBWR, comparisons of the ESBWR and ABWR geometry, and a review of the ABWR HVT FS* testing.

5.4.1   Review of ABWR and ESBWR Containment Geometry

As with CO, it was determined that the pool and horizontal vent geometry for the ESBWR and ABWR are sufficiently similar to allow a direct application of chugging wall pressure amplitudes and wall pressure distributions. Also, as described in Section 4.0 for CO, the differences in plant geometry, which do exist between the two designs, add to the conservatism of this approach.

5.4.2   Review of Thermal-hydraulic Conditions

According to Reference 4, the HVT chugging data support that chugging wall pressure amplitude has some dependence on mass flux and pool temperature, but with substantial randomness. Chugging will occur at the tail end of a LOCA event or for small break accident when low mass flux conditions occur. The ABWR chugging loads were developed to bound the expected range of thermal hydraulic conditions during chugging. Per Reference 4, the highest chugging amplitudes occur with steam breaks with an initially cold pool temperature. This indicates that the limiting conditions occur with colder pool temperatures. Consequently, any potential increase in the pool temperature response introduced by differences between the ESBWR and ABWR does not impact chugging. Additionally, the HVT FS* tests were performed with a pre-purged drywell (steam only condition in the drywell) which provides a bounding condition with respect to nitrogen content relative to the expected ESBWR response. Based on this review of the ABWR chugging load definition basis, it has been determined that the limiting thermal hydraulic conditions during chugging, which affect the chugging wall amplitude for the ESBWR are enveloped by the range of conditions tested in the development of the ABWR chugging load.

5.4.3   Frequency Content Evaluation

The HVT FS* test data show that most of the chugging energy is contained within frequencies associated with pool acoustic modes. This is attributed to the fact that the bubble collapse during chugging occurs predominately outside of the vent, in the suppression pool. Because the ESBWR pool depth is significantly less than the ABWR depth, the chugging wall pressure "ring-out" frequencies, which are associated with the pool acoustic modes, do require adjustment.

From a simple acoustic analysis of a pool with a rigid bottom and a free surface, the fundamental frequency is given in the terms of sound speed in water, c, and pool depth, L, by

$$f = c/4L \qquad\qquad (5\text{-}1)$$

Therefore, to adjust the ABWR chugging frequency to the ESBWR, the ABWR chugging frequency is increased by the ratio of the ABWR pool depth-to-ESBWR pool depth. To accomplish the frequency adjustment, the time scales for the ABWR chugging time histories are compressed by the ratio of the ESBWR pool depth-to-ABWR pool depth when applied to the ESBWR. The ratio is approximately 1/1.3.

5.5   Application of the ABWR Chugging Load to the ESBWR

The pool boundary chugging pressure loads, obtained from analysis of a single-vent sector model of the ABWR prototypical design, are specified for application over the full model of the ESBWR configuration. To bound symmetric and asymmetric loading conditions, two load cases are defined.

1. All vents chugging in phase.
2. Vents in one half chugging 180° out of phase with the other half vents.

For structural analyses, the pool boundary load is specified as a pressure-time history. A total of eight time pool boundary pressure histories, representing different chugging behavior, are specified.

Adjustments for ESBWR Application

Adjustments are made to the ABWR chugging load pressure history amplitude and frequency to add conservatism and to account for the difference in suppression pool depth.

Pressure Amplitude

The chugging pressures determined from the ABWR model calculation are multiplied by a factor of 1.2 to obtain additional conservatism.

Frequency

The time scale is compressed to account for the frequency adjustment described in Section 5.4. The pressures are applied to the pool boundary using the normalized spatial distribution in Figure 5-3.

5.6   Horizontal Vent Loads

The HVT FS* facility was instrumented with two load cells on the top horizontal vent to measure the vertical force and bending moment experienced by the vent during chugging. Chugging has a potential to induce significant loading on the horizontal vent. With the prototypical vent system design, in which the horizontal vents project into the pool, it is anticipated that these anticipated loads may be of significance to containment structure design.

For structural evaluation of the ESBWR containment horizontal vent pipe and pedestal, an upward load, based on the ABWR HVT data, is conservatively defined.

For building structure response analysis and for the evaluation of RPV and its internals, a horizontal vent upward load is specified. To bound symmetrical and asymmetrical loading conditions, the following two load cases are considered and analyzed.

1. Upward load on the pedestal wall simultaneously at all top 12 horizontal vents.
2. Upward load on the pedestal wall simultaneously at top six vents in one-half side of pedestal.

The Horizontal Vent Loads are shown in Figures 5-4 and 5-5 and are applied to the ESBWR with a 1.2 multiplier.

[[   ]]

Figure 5-1. HVT FS* Test Facility
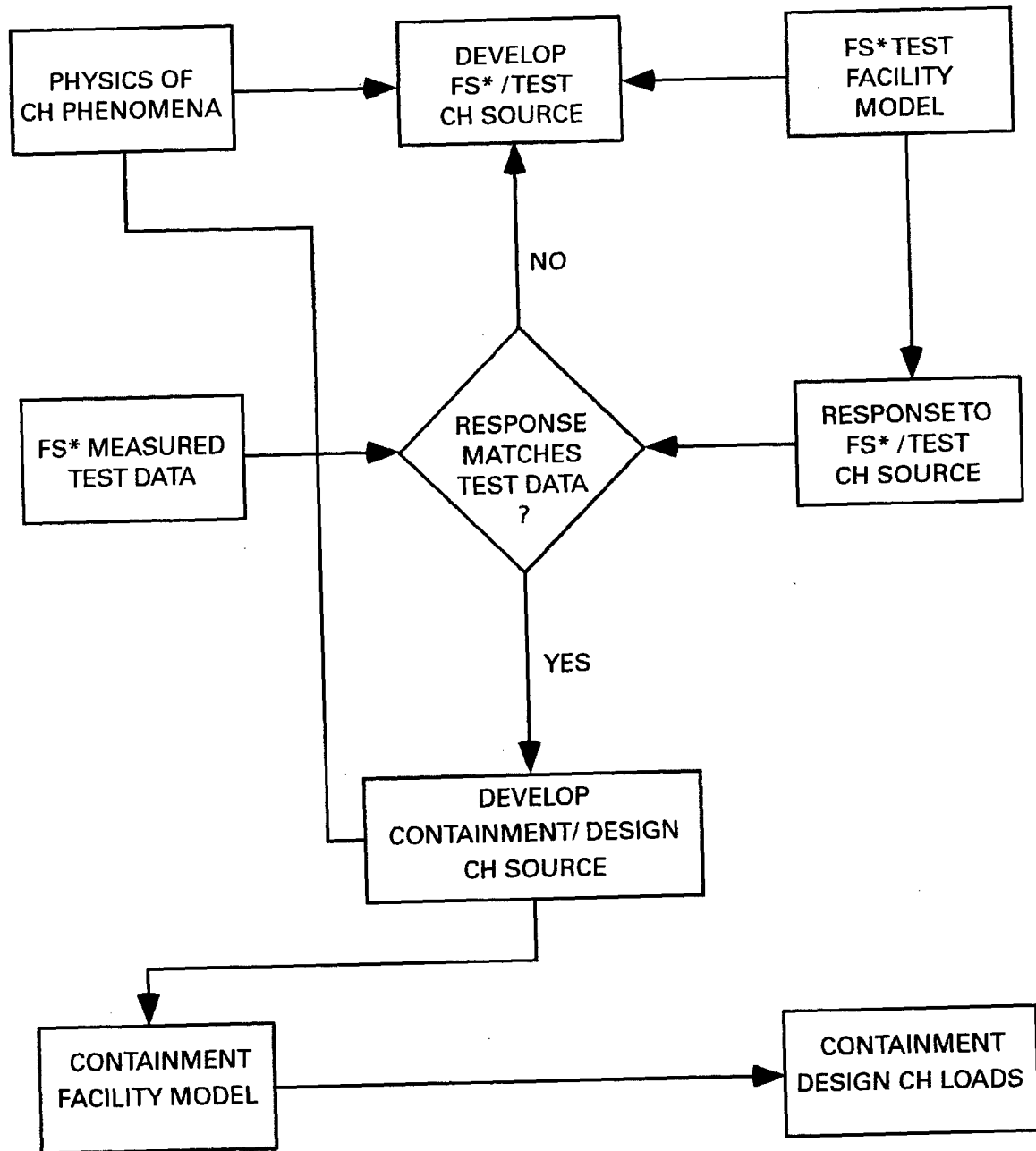
Figure 5-2. Containment CH Source Load Methodology

Figure 5-3. Spatial Load Distribution for CH

[[   ]]

**Figure 5-4. Horizontal Vent Upward Loading for Structure Response
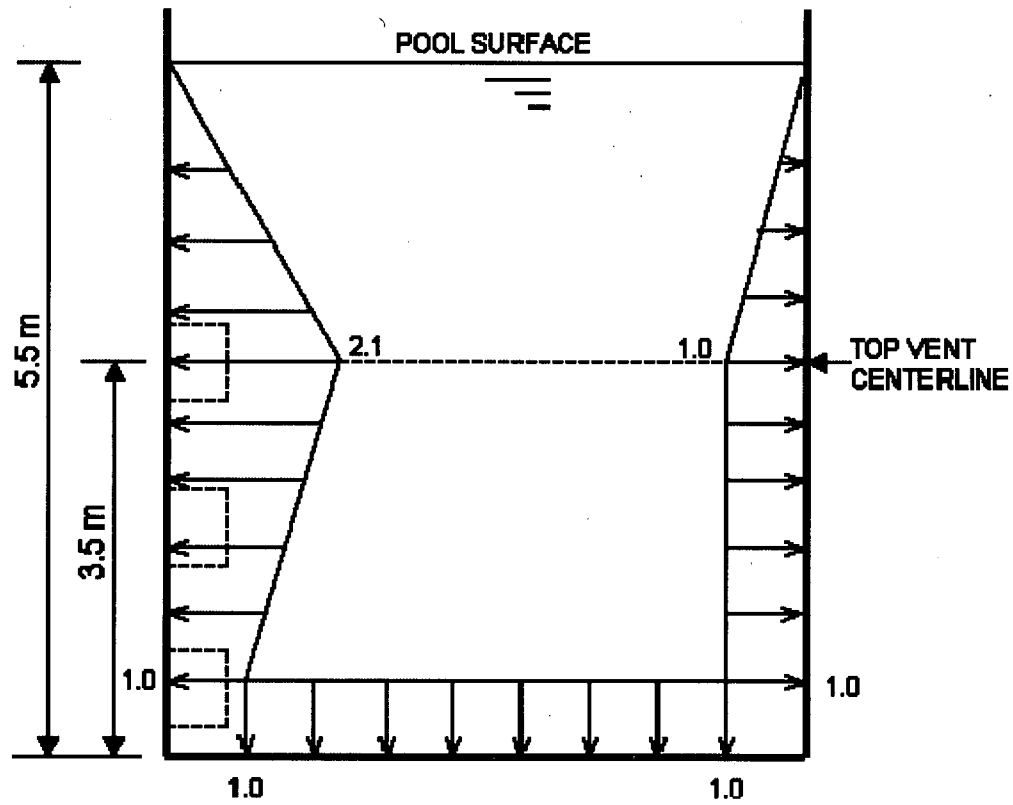Analysis (Apply 1.2 Multiplier to Amplitude for ESBWR)**

[[   ]]

**Figure 5-5. Horizontal Vent Upward Loading for Vent Pipe and Pedestal
(Apply 1.2 Multiplier to Amplitude for ESBWR)**

6.0   SAFETY RELIEF VALVE LOADS

6.1   SRV Design

The ESBWR uses Mark III type X-quenchers in the suppression pool for condensing steam released through the safety relief valves (SRV). During the actuation of a SRV, the nitrogen initially contained inside the discharge line is compressed and subsequently expelled into the suppression pool by the RPV blowdown steam entering the discharge line. The nitrogen exits through holes drilled into an X-quencher device, which is attached to the discharge line. The X-quencher discharge device is utilized in ESBWR to promote effective heat transfer and stable condensation of discharged steam in the suppression pool, thereby minimizing suppression pool boundary loads.

The ESBWR design contains ten Automatic Depressurization System (ADS) safety relief valves.

Each ADS valve is piped to the suppression pool by a discharge line (SRVDL) to an X-quencher in the suppression pool. All ten valves have the same spring setpoint.

6.2   SRV Discharge Load

When a relief valve lifts, the effluent reactor steam causes a rapid pressure build up in the discharge pipe. This rapid compression of the column of nitrogen in the pipe causes a subsequent acceleration of the water slug in the submerged portion of the pipe. During this blowout process the pressure in the pipe builds to a peak as the last of the water is expelled. The compressed cushion of nitrogen between the water slug and the effluent vapor exits the quencher and forms four clouds of small bubbles that begin to expand to the lower pool pressure. This expansion leads to coalescence of the bubble cloud into four bubbles. The four bubbles continue to oscillate, displacing the water and propagating a pressure disturbance throughout the suppression pool. The dynamics of the submerged bubbles are manifested in pressure oscillations arising from the bubble expansion coupled with inertial effects of the moving water mass. The sequence of expansion and contraction is repeated with an identifiable frequency until the bubbles reach the pool surface.

The magnitude of the pressure disturbance in the suppression pool decreases with increasing distance from the point of discharge, resulting in a damped oscillatory load of varying magnitude on structures below the water surface.

After the nitrogen has been expelled, steam exits the quenchers and condenses in the pool. The condensing steam produces negligible (pressure) amplitude loads on the pool boundary, as observed from X-quencher discharge testing.

Calculational methodology for defining the quencher discharge loads for the ESBWR containment is the same as that used for prior ABWR, Mark III, and Mark II containments. Attachment A to Reference 6 provides a detailed description of the calculational methodology. This methodology is based directly on empirical correlations based on and obtained from mini-scale, small-scale, and large-scale (including in-plant) tests conducted to develop a load definition methodology for X-quencher discharge loads during the SRV actuation.

The X-quencher test data were statistically correlated to provide a relationship, which can be used to calculate the magnitude of quencher arm clearing pressure loads on the pool boundary as a function of several key parameters. The correlation was developed for use in both Mark II and Mark III containment systems using X-quencher discharge devices for the SRV lines. Detailed description of (1) the data base, (2) a quantitative assessment of the test data in terms of the physical phenomena, (3) the procedure for identification and justification of key parameters used in the statistical correlations, (4) the statistical analysis of the data, and (5) the resulting correlation equations, are provided in Section A12 of Reference 9.

In summary, the calculational methodology consists of:

- A statistically derived correlation for predicting the magnitude of the peak positive bubble pressure and the relationship for calculating maximum negative pressure from the maximum positive pressure.
- An idealized oscillatory pressure history representing subsequent interaction of the quencher nitrogen bubble with the suppression pool.
- A relationship for determining the pressure field in the suppression pool as a function of distance from the quencher.
- A technique for determining the total nitrogen bubble pool boundary load for subsequent actuation from the first actuation loads, and when more than one quencher bubble exists in the pool (multiple valve actuation conditions).

6.3 Pool Boundary Loads

The absolute pressure on the pool walls due to SRV discharge is calculated by the following equation:

$$P_{(a)} = P_{w/w \text{ gas-space}} + P_h + P_r \tag{6-1}$$

where

$P_{(a)}$	=	Absolute pressure at point (a)
$P_{w/w \text{ gas-space}}$	=	Absolute pressure of wetwell gas-space
P_h	=	Hydrostatic pressure
P_r	=	Bubble pressure attenuated by distance, r to point (a).

The pressure decays with time.

The bubble pressure at point (a) P_r, is calculated from bubble pressure, P_b, using the following relationship.

$$P_r = 2P_b r_0/r : \text{for } r > 2r_0 \qquad (6\text{-}2)$$

$$P_r = P_b : \text{for } r \leq 2r_0$$

where

r_0 = the quencher radius, and

r = the line of sight distance from the quencher center-point to the evaluation point.

Nitrogen bubble pressure loads from a particular quencher location are considered to act only on the boundaries, which can be viewed from the quencher with direct line of sight, as illustrated in Figure 6-1. As an illustration, Figure 6-2 shows the ideal pressure history, which is normalized for the maximum pressure value. This pressure time history profile is used in determining the pressure amplitude variation with time and the number of pressure cycles. It should be noted that the bubble pressure decays to $1/3$ P_{max} within 5 cycles for any frequency between 5 and 12 Hz. The justification for this application is from examination of full-scale plant data where most traces were observed to decay to a small fraction of their peak value in two or three cycles. The design loads consider and include the following SRV actuation cases:

- Single valve discharge for first and subsequent actuations.
- Multiple valve discharge.

The spatial distribution of SRV boundary pressure is shown in Figure 6-3.

6.3.1   Single Valve Discharge

For the ESBWR, single SRV discharge is not a normal operational event. However, the plant is designed for an inadvertent opening of a single valve. Therefore, pressure loadings resulting from both first and subsequent SRV actuations are considered. The SRV lines resulting in the most severe pressure loading are selected for design assessment.

The following major assumptions are made for single valve discharge load definition:

1. Maximum SRV discharge line volumes are used.
2. Suppression pool is at high water level and peak normal operating temperature.
3. SRV setpoints are increased 3% to account for drift and tolerance.

4. The minimum valve opening time is 20 msec.

Nitrogen bubble pressure loads from a particular quencher are considered to act only on boundaries, which can be viewed from the quencher bubble with direct line of sight as illustrated in Figure 6-1.

6.3.2 Multiple Valve Discharge

This case covers the events in which multiple SRVs actuate.

During a postulated LOCA as part of the normal ADS function, five SRVs open when the RPV water level drops below the Level 1 setpoint and another five SRVs open with a preset delay. However, because all of the SRVs have the same setpoint, assuming all SRVs actuate together is a bounding assessment.

In addition to the single valve discharge assumptions, the following assumptions are made for multiple valve discharge load definition:

1. Suppression pool is at an elevated high temperature.
2. All the drywell nitrogen (both upper and lower drywell) has been purged to the wetwell.

Variations in time of actuation, valve opening time and individual discharge line lengths influence the time to complete line clearing, and introduce differences in phasing of the oscillating nitrogen bubbles in the suppression pool. However, these phase differences are neglected, in combining the loads from the individual SRV bubbles.

For multiple valve discharge, the pressure time history, normalized for the maximum pressure value, is shown in Figure 6-2 for a representative frequency of 8 Hz. The maximum positive pressure is given in Table 6-1. The bubble frequency range for analysis is 5 to 12 Hz. Hence, for frequencies other than 8 Hz, the cycle width and length times in Figure 6-2 have to be adjusted accordingly.

As a conservative approach, the multiple valve discharge case considers and includes the most severe symmetric and asymmetric load cases. The most severe symmetric load case assumes oscillating nitrogen bubbles (from all valves) in phase, and the most severe asymmetric case assumes one half of oscillating nitrogen bubbles out of phase with the other half of the oscillating nitrogen bubbles. These two load cases bound all multiple valve actuation cases. The combined pressure loading from multiple valves is obtained by SRSS (Square Root of the Sum of the Squares) of the loads of the single valves acting on the designated evaluation point.

Hence, for multiple SRV actuation the combined bubble pressure load ΔP_r, must be calculated using the following equations:

$$\Delta P_r = \left[\sum_{n=1}^{n} P_n^2 \right]^{1/2} \tag{6-3}$$

where,

$$P_n = 2P_b \left(\frac{r_o}{r_n} \right) \qquad \text{for } r_n > 2r_o$$

$$P_n = P_b \qquad \text{for } r_n \le 2r_o$$

If the calculated $\Delta P_r > P_b$, set $\Delta P_r = P_b$. Note that r_n = the distance from the center of the quencher to point a.

6.3.3 SRV Bubble Pressure (P_b)

The SRV bubble pressure (P_b) is calculated by the methodology described in Section 6.2. Pressures calculated by using this methodology have been shown to be conservative based on previous plant test results (Reference 9). These pressures are based on a 95-95% confidence level of the Caorso data (References 10 and 11).

Bubble pressures are reported below for three major cases:

1. Single Valve First Actuation
2. Single Valve Subsequent Actuation
3. Multiple Valve Actuation

The design limit bubble pressures are reported in Table 6-1.

In order to allow for variations in the ESBWR design, ranges or limits of inputs used to calculate the SRVDL air clearing loads are defined. These ranges and limits constitute constraints, which must be adhered to, in order to avoid exceeding the SRV X-Quencher loads defined in Table 6-1.

The constraints are as follows:

Geometric and Thermal-Hydraulic Constraints:

Maximum SRVDL Air Volume:	$1.675 m^3$	
Corresponding SRVDL Air Column Length (L_A):	$25m < L_A < 36m$	(pipe ID = 0.243m.)
SRVDL Submerged Line Length (L_S):	$2\ m < L_S < 5\ m$	(pipe ID = 0.243m)
SRV Rated Capacity:	< 144 kg/sec	(at 8877 kPa g)

Suppression Pool Temperature (T_P): $T_P < 48.9°C$ (RPV at rated pressure)

                                          $T_P < 80°C$ (RPV at low pressure)

SRV Opening Time (V_{OT}): $20 \text{ ms} < V_{OT} < 1700 \text{ ms}$

Suppression Pool Water Surface Area: $> 799 \text{ m}^2$

SRV Quencher Area: $< 6.936 \text{ m}^2$

Event-Based Constraints:

The acceptability of the SRVDL air clearing loads are predicated on:

- Final RPV depressurization from rated pressure initiated before the suppression pool exceeds 120°F (48.9°C),
- Only one actuation of multiple SRVs at RPV high pressure,
- No subsequent actuation of multiple SRVs at any time, and
- No subsequent actuation of SRVs (single or multiple) during high RPV pressure with high containment pressure and high suppression pool temperature conditions.

6.3.4   Quencher Steam Condensation Loads

Previous test data (References 10 and 11) indicate negligible condensation loads for quencher devices. Additional data provided in Reference 12, demonstrates that condensation loads over the full range of pool temperatures up to saturation, are low compared to loads due to SRV discharge, Condensation Oscillation, and chugging, which is considered in containment design evaluation.

Hence, dynamic loads during quencher steam condensation process are not defined here nor considered for containment evaluation.

Table 6-1. SRV Bubble Pressure

	Design Value
Peak Positive Pressure (kPa d)	
• Single Valve First Actuation	91
• Single Valve Subsequent Actuation	152
• Multiple Valves	76
Peak Negative Pressure (kPa d)	
• Single Valve First Actuation	54
• Single Valve Subsequent Actuation	63
• Multiple Valves	54

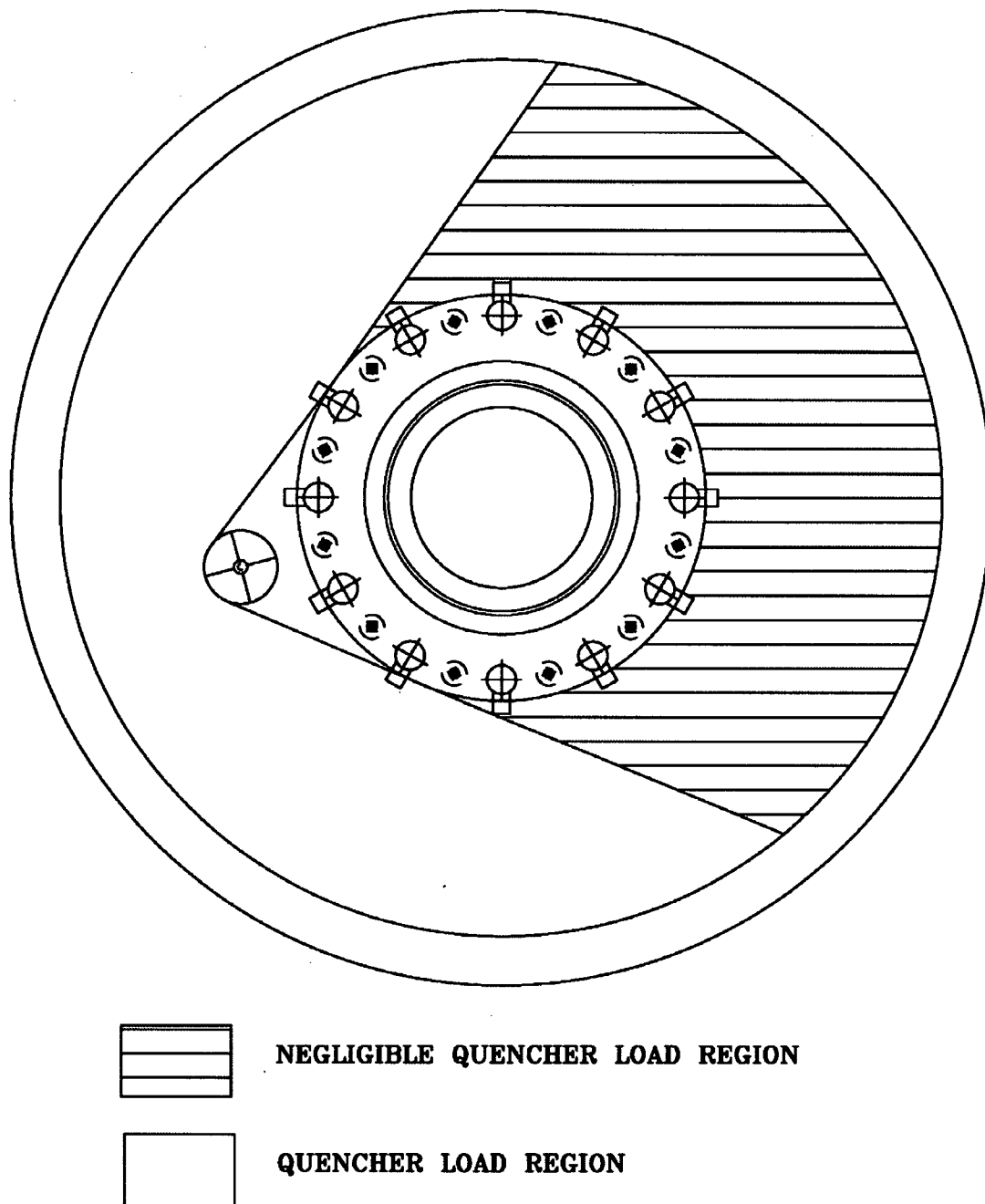**NEGLIGIBLE QUENCHER LOAD REGION**

QUENCHER LOAD REGION

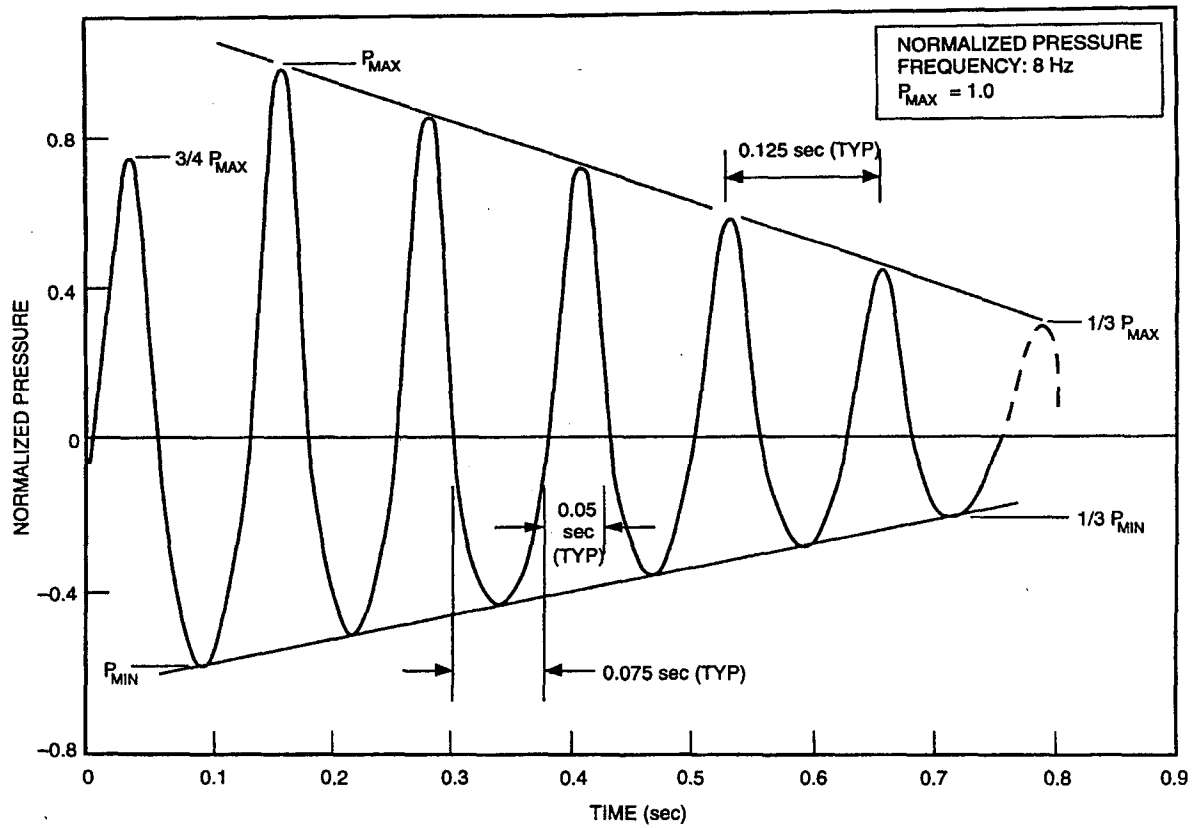**Figure 6-1. Load Distribution Region of Influence**

Figure 6-2. Normalized Quencher Bubble Pressure Time History (Ideal)
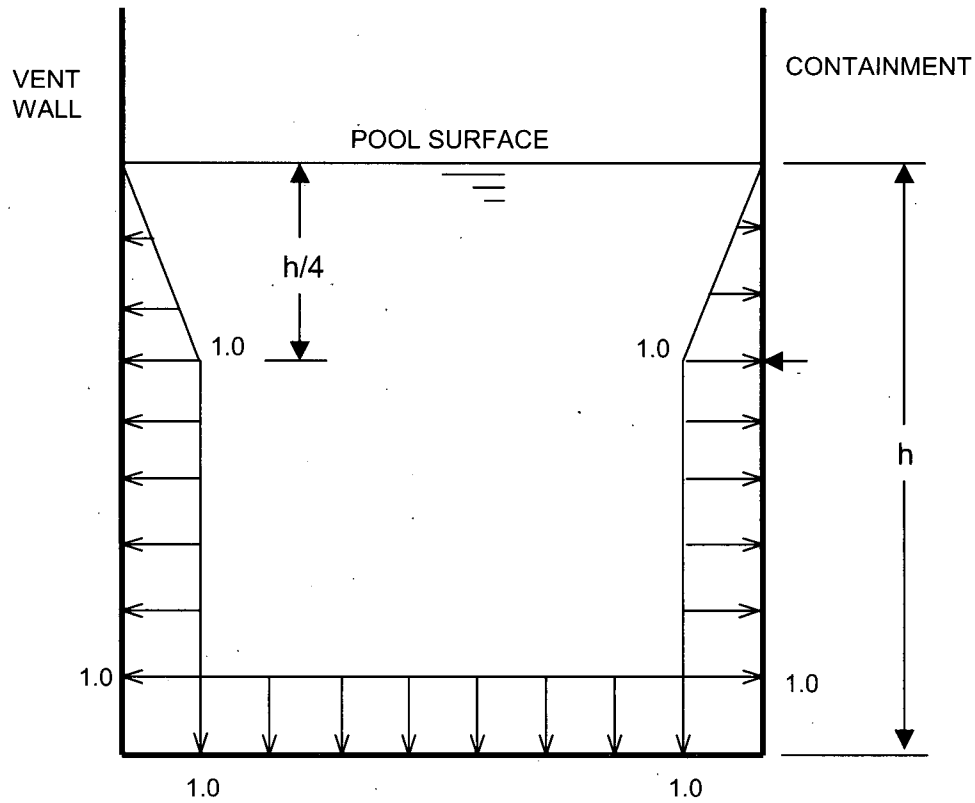
Figure 6-3. SRV Boundary Pressure Spatial Distribution, Normalized to Maximum Pressure Amplitude

7.0   ESBWR UNIQUE DESIGN FEATURES

7.1   Passive Containment Cooling System

The PCCS receives a steam-gas mixture supply directly from the drywell; it does not have any valves, so it immediately starts into operation, following a LOCA event. Nitrogen, together with steam vapor, enter the PCCS condenser; steam is condensed inside PCCS condenser vertical tubes; and the condensate, which is collected in the lower headers, is discharged to the GDCS pool. The nitrogen is purged to the wetwell through the vent line, which is submerged in the suppression pool.

7.1.1   PCCS Pool Swell Loads

Pool swell loads caused by PCCS vent discharge are not significant because of the following:

1.   The PCCS pipe area is significantly smaller than the main vent area.
2.   The PCCS vent submergence is less than the main vents.

Consequently, the main vent pool swell loads presented in Section 3.0 are the bounding loads.

7.1.2   PCCS Condensation Loads

Condensation Oscillation (CO) for the main vent system is described in Section 4.0. CO may also be present at the PCCS vent exit during a LOCA when a nitrogen-steam mixture is discharged from the condenser and the resultant steam is condensed in the suppression pool. However, because the diameter of the PCCS vent line is significantly smaller than the diameter of a main horizontal vent, the mass flow rate through the main vents during a DBA-LOCA would be significantly higher than the mass flow rate through the PCCS vents, and the CO loads derived for the main vent system would bound any CO loads resulting from the PCCS vent discharge. Consequently, CO loads presented in Section 4.0 are the bounding loads.

Chugging at the vent discharge is prevented by the presence of the PCCS condenser. In order to have chugging at the PCCS vent exit, the amount of nitrogen in the mixture must be small or absent. Because the flow from the drywell to the suppression pool must first pass through the condenser tubes, most or all of the steam would be condensed. The resultant mixture would have a high concentration of nitrogen sufficient that chugging at the vent exit would not occur.

7.2   Gravity-Driven Cooling System

The GDCS pools are equipped with spillover pipes (scuppers) that are piped to the main vent entrance. This is to ensure that any overflow (by PCC condensate for example) goes to the

suppression pool rather than spilling on the upper DW floor and finding its way to the lower drywell. While these drainpipes have yet to be designed, they are not expected to have any impact on the containment thermal-hydraulic loads.

At the start of any LOCA, both ends of the pipe are exposed to the drywell airspace and, hence, have the same pressure. Therefore, the drainpipe does not affect the pool swell blowdown flow through the main vent system.

Later during the transient, the PCCS condensate adds water to the GDCS tanks. However, the GDCS will actuate before the water level reaches the spillover pipe, and the tanks will drain into the RPV. Therefore, these spillover pipes will not have flow during design basis events and, thus, have no impact on the main vent performance.

7.3   Lower Drywell Spillover Pipes

The twelve lower drywell spillover pipes have been replaced with small pipes directly connected to the main vents above the pool water line. This design does not have any impact on the containment thermal-hydraulic loads.

7.4   Depressurization Valves

The impact of depressurization valve (DPV) actuation is discussed in Section 2.3. The DPV loads are bounded by the DBA LOCA loads.

8.0 SUBMERGED STRUCTURE LOADS

Structures submerged in the suppression pool can be subjected to flow induced hydrodynamic loads due to a LOCA and/or SRV/DPV actuations.

During a LOCA, a steam/water mixture rapidly escapes from the break, and the drywell is rapidly pressurized. The water initially in the vent system is expelled out into the suppression pool. A highly localized induced flow field is created in the pool and a dynamic loading is induced on any submerged structures. After the water is expelled from the vent system, the nitrogen initially in the drywell is forced out through the horizontal vents into the suppression pool. The nitrogen exiting from the vents forms expanding bubbles, which create moderate dynamic loads on structures submerged in the pool. The nitrogen bubbles cause the pool water surface to rise until they break through the pool water surface. The pool surface water slug decelerates and falls back to the original pool level as the steam/water mixture from the break fills the drywell and is channeled to the pool via the vent system. Steam condensation starts and the oscillatory nature of the phenomena causes a vibratory load on submerged structures. The Condensation Oscillation (CO) loading continues until the pressure in the drywell decreases. A less regular condensation loading called chugging (CH) follows this. During the CH period, a high frequency spike is propagated and causes an acoustic loading on submerged structures.

During SRV actuations, the dynamic process is quite similar to LOCA steam blowdown except that the X-quencher attached at the discharge end mitigates the induced load. Two types of loads are important. One is due to the water jet formed at the X-quencher arm discharge, and the second is due to the four gas bubbles formed between the arms of the X-quencher. These bubbles are smaller in size than the LOCA bubbles, reside longer in the pool and oscillate as they rise to the free surface of the suppression pool.

8.1 Pool Swell Submerged Structure Loads

During the initial phase of the DBA, the drywell is pressurized and the water in the vents is expelled to the pool and induces a flow field throughout the suppression pool. This induced flow field creates a dynamic load on structures submerged in the pool. For submerged structures that are not in the direct path of these jets, the dynamic load on these structures is less than the load induced by the LOCA gas bubble that forms after the water is expelled. Because the gas bubble induced dynamic load is bounding, this load is conservatively used in place of the water jet load. For submerged structures that are in the direct path of these jets, water jet loads are compared with bubble dynamic loads, and the higher load used.

After the vents are cleared of initially contained water, pressurized drywell nitrogen is purged into the suppression pool, and a single bubble is formed around each vent exit. It is during the bubble growth period that unsteady fluid motion is created within the suppression pool. During this period, all submerged structures below the pool surface are exposed to transient hydrodynamic loads.

The load definition methodology for defining the LOCA bubble induced loads on submerged structures is consistent with the methodology used for prior plants, as described in Reference 13.

8.2 CO Submerged Structure Loads

During LOCA, after the vent has been cleared of water and the drywell nitrogen has been carried over into the wetwell, steam condensation begins. This CO phase induces bulk water motion and, therefore, creates drag loads on the structures submerged in the pool.

The load definition methodology for defining the LOCA steam CO loads on submerged structures is consistent with the methodology used for prior plants. The methodology is described in Reference 14.

8.3 CH Submerged Structure Loads

CH occurs after the drywell nitrogen has been purged and carried over into the wetwell, and the vent steam mass flux falls below a critical value. CH then induces acoustic pressure loads on structures submerged in the suppression pool. The load definition methodology for defining the LOCA CH loads on submerged structures is consistent with methodology used for prior plants. This methodology is described in Reference 14.

8.4 SRV Submerged Structure Load

Following the actuation of the SRVs, water contained initially in the line is rapidly purged through the X-quencher attached at the end of the SRV discharge line. A highly localized water jet is formed around the X-quencher arms. The hydrodynamic load, due to the water jet outside a sphere circumscribed around the quencher arms, is conservatively bounded by the gas bubble induced dynamic load. There are no submerged structures located within the sphere mentioned above in the ESBWR arrangement.

After the water discharge, the nitrogen initially contained in the discharge line is forced into the suppression pool under high pressure. The gas bubbles that are formed interact with the surrounding water and produce oscillating pressure and velocity fields in the suppression pool. This pool disturbance gives rise to hydrodynamic loads on submerged structures in the pool.

The load definition methodology for defining the SRV bubble loads on submerged structures is consistent with that used for prior plants. This methodology is described in References 13 and 15.

8.5   PCCS Vent Discharge Load

The load definition methodology for defining the PCCS non-condensable vent discharge loads on submerged structures is similar to the methodology defined in Section 8.4 for SRV loads. However, the SRV loads bound the PCCS vent discharge load.

9.0 LOAD COMBINATIONS

Under certain plant conditions, the containment structures can be subjected simultaneously to hydrodynamic loads due to a LOCA event (DBA, IBA or SBA) and SRV actuations. Figure 9-1 shows the combination history of these loads for the controlling DBA-LOCA events. The chart shows the time intervals when specific loads could occur. At any given time on the chart, the containment structures may experience all the loading conditions in those boxes, which span that time. However, the loads may not be continuous over the entire range depicted in the chart, especially the SRV and CH loads.

Event-time relationships showing load combination histories for design assessment of the ESBWR containment system are, in general, consistent with the approach used for other BWR plants including ABWR (Reference 1).

DBA PRESSURE / TEMPERATURE LOADS

SAFETY RELIEF VALVE LOADS

PS

CO

CH

T₁   T₂   72 hr
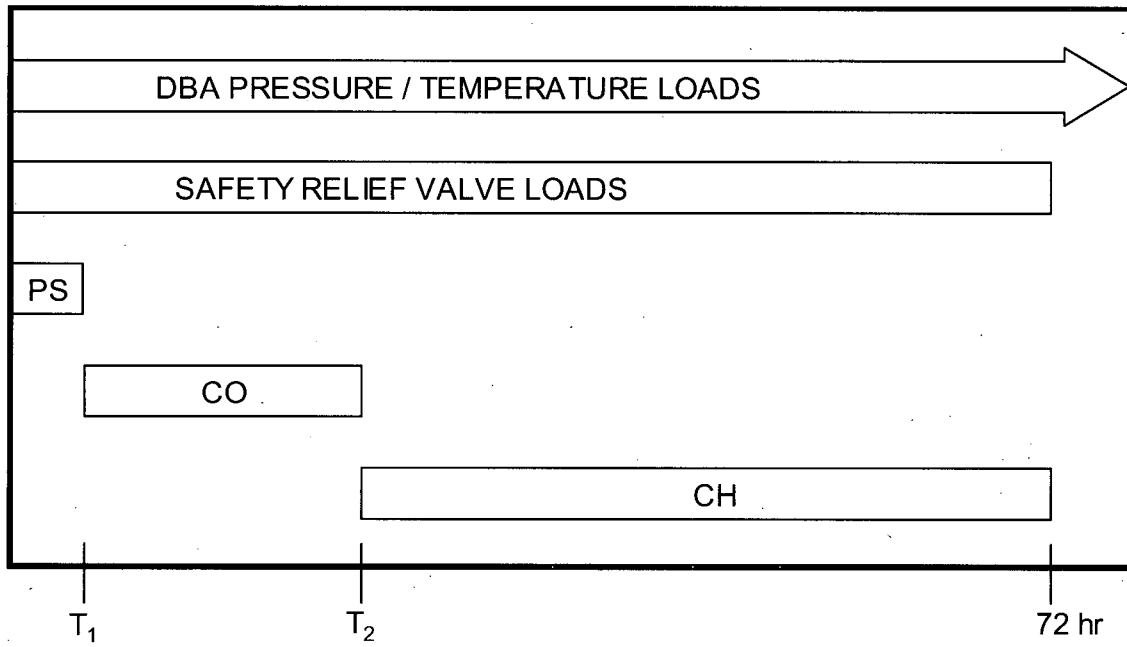
	T₁	T₂
MSLB	[[	]]
FWLB	[[	]]

Figure 9-1. Time Relationship for a DBA-LOCA

10.0 REFERENCES

[1] General Electric Company, "Advanced Boiling Water Reactor, Standard Safety Analysis Report," 23A6100, Class III (Proprietary) and Class I (Non-proprietary), Revision 8, May 13, 1996 (Appendix 3B, Containment Hydrodynamic Loads).

[2] General Electric Company, "The General Electric Mark III Pressure Suppression Containment Analytical Model," NEDO-20533, Class I (Non-proprietary), Revision 0, June 1974.

[3] General Electric Company, "Mark II Pressure Suppression Containment Systems: An Analytical Model of the Pool Swell Phenomenon," NEDE-21544-P, Class III (Proprietary), Revision 0, December 1976, and NEDO-21544, Class I (Non-proprietary), Revision 0, December 1976.

[4] General Electric Company, "Containment Horizontal Vent Confirmatory Test, Part I," NEDC-31393, Class III (Proprietary), Revision 0, March 1987.

[5] General Electric Company, "Scaling Study of the General Electric Pressure Suppression Test Facility, Mark III Long-Range Program, Task 2.2.1," NEDE-25273, Class III (Proprietary), Revision 0, March 1980.

[6] General Electric Company, "GESSAR II, BWR/6 Nuclear Island Design," 22A7007, Class III (Proprietary) and Class I (Non-proprietary), Revision 19, May 28, 1985 (Appendix 3B, Containment Hydrodynamic Loads).

[7] General Electric Company, "Mark III Confirmatory Test Program - 1/√3 Scale Condensation and Stratification Phenomena – Test Series 5807," NEDE-21596-P, Class III (Proprietary), Revision 0, March 1977, and NEDO-21596, Class I (Non-proprietary), Revision 0, March 1977.

[8] General Electric Company "Mark II Containment Program, Generic Chugging Load Definition Report," NEDE-24302-P, Class III (Proprietary), Revision 0, April 1981, and NEDO-24302, Class I (Non-proprietary), Revision 0, July 1981.

[9] General Electric Company, "Containment Loads Report (CLR), Mark III Containment," 22A4365AB, Class III (Proprietary), Revision 4, January 25, 1980, and 22A4365, Class I (Non-proprietary), Revision 0, January 25, 1980.

[10] General Electric Company, "Mark II Containment Supporting Program, Caorso Safety Relief Valve Discharge Tests, Phase I Test Report," NEDE-25100-P, Class III (Proprietary), Revision 0, May 1979, NEDO-25100, Class I (Non-proprietary), Revision 0, August 1979, and NEDO-25100-EA, Class I (Non-proprietary), Revision 0, February 1981.

[11] General Electric Company, "Mark II Containment Supporting Program, Caorso Safety Relief Valve Discharge Tests, Phase II Apparent Test Results Report," NEDE-25118, Class III (Proprietary), Revision 0, August 1979.

10.0 REFERENCES

[12] General Electric Company, "Elimination of Limit on BWR Suppression Pool Temperature for SRV Discharge With Quenchers," NEDO-30832-A, Class I (Non-proprietary), Revision 0, May 1995.

[13] General Electric Company, "Analytical Model for Estimating Drag Forces on Rigid Submerged Structures caused by LOCA and Safety Relief Valve Ramshead Air Discharges," NEDO-21471, Class I (Non-proprietary), Revision 0, September 1977.

[14] General Electric Company, "Analytical Model for Estimating Drag Forces on Rigid Submerged Structures Caused by Steam Condensation and Chugging, Mark III Containments" NEDO-25153, Class I (Non-proprietary), Revision 0, July 1979.

[15] General Electric Company, "Analytical Model for Estimating Drag Forces on Rigid Submerged Structures Caused by LOCA and Safety Relief Valve Ramshead Air Discharges, Supplement for X-Quencher Air Discharges," NEDO-21471-01, Class I (Non-proprietary), Revision 0, October 1979.

[16] USNRC Report NUREG-0978, "Mark III LOCA-Related Hydrodynamic Load Definition," August 1984.

Enclosure 3

MFN 07-563

AFFIDAVIT

GE Hitachi Nuclear Energy

AFFIDAVIT

I, David H. Hinds, state as follows:

(1) I am the General Manager, New Units Engineering, GE Hitachi Nuclear Energy ("GEH") and have been delegated the function of reviewing the information described in paragraph (2) which is sought to be withheld, and have been authorized to apply for its withholding.

(2) The information sought to be withheld is contained in Enclosure 1 of GEH letter MFN 07-563, Mr. James C. Kinsey to U.S. Nuclear Regulatory Commission, *Transmittal of Licensing Topical Report (LTR) NEDE-33261P, "ESBWR Containment Load Definition," Revision 1, October 2007, and NEDO-33261, "ESBWR Containment Load Definition," Revision 1, October 2007,* dated November 8, 2007. GEH proprietary information is identified in Enclosure 1, *MFN 07-563 - Licensing Topical Report (LTR) NEDE-33261P, "ESBWR Containment Load Definition," Revision 1, October 2007 - GEH Proprietary Information,* by a dotted underline inside double square brackets. The electronic version includes a dark red font inside the brackets. For black-grayscale printed copies, the red font and dotted underline appears similar to normal text. [[This sentence is an example.{3}]] Figures and large equation objects are identified with double square brackets before, and after the object. In each case, the superscript notation {3} refers to paragraph (3) of this affidavit, which provides the basis of the proprietary determination. Specific information that is not so marked is not GEH proprietary. A non-proprietary version of this information is provided in Enclosure 2, *MFN 07-563 - Licensing Topical Report (LTR) NEDO-33261, "ESBWR Containment Load Definition," Revision 1, October 2007 - Non-Proprietary Information.*

(3) In making this application for withholding of proprietary information of which it is the owner, GEH relies upon the exemption from disclosure set forth in the Freedom of Information Act ("FOIA"), 5 USC Sec. 552(b)(4), and the Trade Secrets Act, 18 USC Sec. 1905, and NRC regulations 10 CFR 9.17(a)(4), and 2.390(a)(4) for "trade secrets" (Exemption 4). The material for which exemption from disclosure is here sought also qualify under the narrower definition of "trade secret", within the meanings assigned to those terms for purposes of FOIA Exemption 4 in, respectively, <u>Critical Mass Energy Project v. Nuclear Regulatory Commission,</u> 975F2d871 (DC Cir. 1992), and <u>Public Citizen Health Research Group v. FDA,</u> 704F2d1280 (DC Cir. 1983).

(4) Some examples of categories of information which fit into the definition of proprietary information are:

a. Information that discloses a process, method, or apparatus, including supporting data and analyses, where prevention of its use by GEH's competitors without license from GEH constitutes a competitive economic advantage over other companies;

b. Information which, if used by a competitor, would reduce his expenditure of resources or improve his competitive position in the design, manufacture, shipment, installation, assurance of quality, or licensing of a similar product;

c. Information which reveals aspects of past, present, or future GEH customer-funded development plans and programs, resulting in potential products to GEH;

d. Information which discloses patentable subject matter for which it may be desirable to obtain patent protection.

The information sought to be withheld is considered to be proprietary for the reasons set forth in paragraphs (4)a., and (4)b, above.

(5) To address 10 CFR 2.390(b)(4), the information sought to be withheld is being submitted to NRC in confidence. The information is of a sort customarily held in confidence by GEH, and is in fact so held. The information sought to be withheld has, to the best of my knowledge and belief, consistently been held in confidence by GEH, no public disclosure has been made, and it is not available in public sources. All disclosures to third parties including any required transmittals to NRC, have been made, or must be made, pursuant to regulatory provisions or proprietary agreements which provide for maintenance of the information in confidence. Its initial designation as proprietary information, and the subsequent steps taken to prevent its unauthorized disclosure, are as set forth in paragraphs (6) and (7) following.

(6) Initial approval of proprietary treatment of a document is made by the manager of the originating component, the person most likely to be acquainted with the value and sensitivity of the information in relation to industry knowledge, or subject to the terms under which it was licensed to GEH. Access to such documents within GEH is limited on a "need to know" basis.

(7) The procedure for approval of external release of such a document typically requires review by the staff manager, project manager, principal scientist or other equivalent authority, by the manager of the cognizant marketing function (or his delegate), and by the Legal Operation, for technical content, competitive effect, and determination of the accuracy of the proprietary designation. Disclosures outside GEH are limited to regulatory bodies, customers, and potential customers, and their agents, suppliers, and licensees, and others with a legitimate need for the information, and then only in accordance with appropriate regulatory provisions or proprietary agreements.

(8) The information identified in paragraph (2), above, is classified as proprietary because it identifies the models and methodologies GEH will use in evaluating the consequences of design basis accidents (DBAs) for the ESBWR. GEH and its

partners performed significant additional research and evaluation to develop a basis for these revised methodologies to be used in evaluating the ESBWR over a period of several years at a cost of over one million dollars.

The development of the evaluation process along with the interpretation and application of the analytical results is derived from the extensive experience database that constitutes a major GEH asset.

(9) Public disclosure of the information sought to be withheld is likely to cause substantial harm to GEH's competitive position and foreclose or reduce the availability of profit-making opportunities. The information is part of GEH's comprehensive BWR safety and technology base, and its commercial value extends beyond the original development cost. The value of the technology base goes beyond the extensive physical database and analytical methodology and includes development of the expertise to determine and apply the appropriate evaluation process. In addition, the technology base includes the value derived from providing analyses done with NRC-approved methods.

The research, development, engineering, analytical and NRC review costs comprise a substantial investment of time and money by GEH.
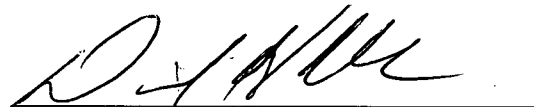
The precise value of the expertise to devise an evaluation process and apply the correct analytical methodology is difficult to quantify, but it clearly is substantial.

GEH's competitive advantage will be lost if its competitors are able to use the results of the GEH experience to normalize or verify their own process or if they are able to claim an equivalent understanding by demonstrating that they can arrive at the same or similar conclusions.

The value of this information to GEH would be lost if the information were disclosed to the public. Making such information available to competitors without their having been required to undertake a similar expenditure of resources would unfairly provide competitors with a windfall, and deprive GEH of the opportunity to exercise its competitive advantage to seek an adequate return on its large investment in developing these very valuable analytical tools.

I declare under penalty of perjury that the foregoing affidavit and the matters stated therein are true and correct to the best of my knowledge, information, and belief.

Executed on this 8th day of November 2007.

David H. Hinds
GE Hitachi Nuclear Energy